

INTERMITTENT PROCESS ANALYSIS WITH SCATTERING MOMENTS

BY JOAN BRUNA[†], STÉPHANE MALLAT^{‡,*}, EMMANUEL
BACRY[§], AND JEAN-FRANÇOIS MUZY^{§,¶}

New York University[†] *École Normale Supérieure*[‡] *CNRS, Ecole
Polytechnique*[§] and *CNRS, Université de Corse*[¶]

Scattering moments provide non-parametric models of random processes with stationary increments. They are expected values of random variables computed with a non-expansive operator, obtained by iteratively applying wavelet transforms and modulus non-linearities, which preserves the variance. First and second order scattering moments are shown to characterize intermittency and self-similarity properties of multiscale processes. Scattering moments of Poisson processes, fractional Brownian motions, Lévy processes and multifractal random walks are shown to have characteristic decay. The Generalized Method of Simulated Moments is applied to scattering moments to estimate data generating models. Numerical applications are shown on financial time-series and on energy dissipation of turbulent flows.

1. Introduction. Defining non-parametric models of non-Gaussian stationary processes remains a core issue of probability and statistics. Computing polynomial moments is a tempting strategy which suffers from the large variance of high order moment estimators. Image and audio textures are examples of complex processes with stationary increments, which can be discriminated from a single realization by the human brain. Yet, the amount of samples is often not sufficient to reliably estimate polynomial moments of degree more than 2. These non-Gaussian processes often have a long range dependency, and some form of intermittency generated by randomly distributed burst of transient structures at multiple scales. Intermittency, is an ill-defined mathematical notion, which is used in physics to describe irregular burst of large amplitude variations, appearing for exemple in turbulent flows [?]. Multiscale intermittency appear in other domains such as network traffics, financial time series, geophysical and medical data.

Intermittency is created by heavy tail processes, such as Levy processes. It produces large if not infinite polynomial moments of degree larger than two, and empirical estimations of second order moments have a large variance.

*This work is supported by the ANR 10-BLAN-0126 and ERC InvariantClass 320959 grants.

These statistical instabilities can be reduced by calculating expected values of non-expansive operators in mean-square norm, which reduce the variance empirical estimations. Scattering moments are computed with such a non-expansive operator. They are calculated by iteratively applying wavelet transforms and modulus non-linearities [22]. This paper shows that they characterize self-similarity and intermittency properties of processes with stationary increments. These properties are studied by computing the scattering moments of Poisson processes, fractional Brownian motions, Levy processes and multifractal cascades, which all have very different behaviors. Scattering moments provide non parametric descriptors which reveal complex statistical properties of time series. The generalized method of simulated moments [14, 26] applied to scattering moments gives a parameter estimator for data generating models. Besides parameter estimation, a key challenge is to validate data generating models from limited data sets. Keeping sufficiently high order scattering coefficients provides a number of scattering moments which is larger than the dimensionality of the model parameter. Confidence levels for model validation can thus be computed with a χ^2 J-test [14].

Section 2 reviews the scaling properties of wavelet polynomial moments for fractal and multifractal processes. Scattering moments are defined and related to multiscale intermittency properties. Poisson processes illustrate these first results. Section 3 proves that self-similar processes with stationary increments have normalized scattering moments which are stationary across scales. Gaussian processes are discriminated from non-Gaussian processes from second order scattering moments. Results on fractional Brownian motion and stable Levy processes illustrate the analysis of multiscale intermittency properties. Section 4 extends these results to self-similar multifractal cascades [23, 24, 5].

Section 5 applies scattering moments to model parameter estimations. It introduces a scattering moment estimator whose variance is bounded. Parameters of data generating models are estimated from scattering moments with the generalized method of simulated moments [14, 26]. Scattering moments of financial time-series and turbulence energy dissipation are computed from numerical data. Models based on fractional Brownian, Levy stable and multifractal cascade processes are evaluated with a J-test. Computations can be reproduced with a software available at www.di.ens.fr/data/software/scatnet.

Notations: We denote $\{X(t)\}_t \stackrel{d}{=} \{Y(t)\}_t$ the equality of all finite-dimensional distributions. The dyadic scaling of $X(t)$ is written $L_j X(t) = X(2^{-j}t)$. If $X(t)$ is stationary then $\mathbf{E}(X(t))$ does not depend on t and is written $\mathbf{E}(X)$, and $\sigma^2(X) = \mathbf{E}(|X|^2) - \mathbf{E}(X)^2$. We denote $B(j) \simeq F(j)$, $j \rightarrow \infty$ (resp

$j \rightarrow -\infty$) if there exists $C_1, C_2 > 0$ and $J \in \mathbb{Z}$ such that $C_1 \leq \frac{B(j)}{F(j)} \leq C_2$ for all $j > J$ (resp for all $j < J$).

2. Scattering Transform of Intermittent Processes.

2.1. *Polynomial Wavelet Moments.* Polynomial moments of wavelet coefficients reveal important multiscaling properties of fractals and multifractals [3, 32, 16, 15, 1, 29, 28, 39, 40]. We consider real valued random processes $X(t)$ having stationary increments $X(t) - X(t - \tau)$ for any $\tau \in \mathbb{R}$. A wavelet $\psi(t)$ is a function of zero average $\int \psi(t) dt = 0$ with $|\psi(t)| = O((1 + |t|^2)^{-1})$, which is dilated:

$$\forall j \in \mathbb{Z} \quad , \quad \psi_j(t) = 2^{-j} \psi(2^{-j} t) .$$

The wavelet transform of $X(t)$ at a scale 2^j is defined for all $t \in \mathbb{R}$ by

$$(1) \quad X \star \psi_j(t) = \int X(u) \psi_j(t - u) du .$$

A wavelet $\psi(t)$ is said to have q vanishing moments if $\int t^k \psi(t) dt = 0$ for $0 \leq k < q$. Since $\int \psi(t) dt = 0$, if X has stationary increments then one can verify that $X \star \psi_j(t)$ is a stationary process [32]. The dyadic wavelet transform of $X(t)$ is:

$$(2) \quad WX = \{X \star \psi_j\}_{j \in \mathbb{Z}} .$$

A wavelet ψ satisfies the Littlewood-Paley condition if its Fourier transform Ψ satisfies for all $\omega \neq 0$:

$$(3) \quad \sum_{j=-\infty}^{\infty} |\Psi(2^j \omega)|^2 + \sum_{j=-\infty}^{\infty} |\Psi(-2^j \omega)|^2 = 2 .$$

If $X(t)$ is a real valued stationary process with $\mathbf{E}(|X(t)|^2) < \infty$ then the wavelet transform energy equals the process variance $\sigma^2(X)$:

$$(4) \quad \mathbf{E}(\|WX\|^2) = \sum_{j \in \mathbb{Z}} \mathbf{E}(|X \star \psi_j|^2) = \sigma^2(X) .$$

This is proved by expressing $\mathbf{E}(|X \star \psi_j|^2)$ from the power spectrum of X and inserting (3).

For random processes $X(t)$, the decay of monomial wavelet moments across scales can be related to the distributions of singularities [3, 32, 16, 39, 40]. Moments of degree q define a scaling exponents $\zeta(q)$ such that

$$\mathbf{E}(|X \star \psi_j(t)|^q) \simeq 2^{j\zeta(q)} .$$

Monofractals such as fractional Brownian motions have linear scaling exponents: $\zeta(q) = q\zeta(1)$. These Gaussian processes have realizations which are uniformly regular. The curvature of $\zeta(q)$ is related to the presence of singularities having different Holder exponents, in each realization of X [15, 29]. It has been interpreted as a measurement of intermittency [1]. However, as q deviates from 1, estimations of moments become progressively more unstable which limits the application of this multifractal formalism to very large data sets.

2.2. Scattering Moments. Scattering moments are expected values of a non-expansive transformation of the process. They are computed with a cascade of wavelet transforms and modulus non-linearities [22]. We review their elementary properties.

Let ψ be a \mathbf{C}^1 , complex wavelet, whose real and imaginary parts are orthogonal, and have the same $\mathbf{L}^2(\mathbb{R})$ norm. In this paper we impose that ψ has a compact support normalized to $[-1/2, 1/2]$, which simplifies the proofs. However, most results remain valid without this compact support hypothesis. We consider wavelets ψ which are nearly analytic, in the sense that their Fourier transform $\Psi(\omega)$ is nearly zero for $\omega < 0$. The compact support hypothesis prevents it from being strictly zero. All numerical computations in the paper are performed with the compactly supported complex wavelets of Selesnick [36], whose real and imaginary parts have 4 vanishing moments and are nearly Hilbert transform pairs.

Let $X(t)$ be a real valued process with stationary increments having finite first order moments: $\mathbf{E}(|X(t) - X(t - \tau)|) < \infty$ for all $\tau \in \mathbb{R}$. The wavelet transform $X \star \psi_{j_1}(t)$ is a complex stationary random process. First order scattering moments are defined by

$$\forall j_1 \in \mathbb{Z} \quad , \quad \overline{S}X(j_1) = \mathbf{E}(|X \star \psi_{j_1}|) .$$

First order scattering moments do not capture the time variability of wavelet coefficients $X \star \psi_{j_1}(t)$. This information is partly provided by second order scattering moments computed from the wavelet transform of each $|X \star \psi_{j_1}(t)|$:

$$\forall (j_1, j_2) \in \mathbb{Z}^2 \quad , \quad \overline{S}X(j_1, j_2) = \mathbf{E}(|X \star \psi_{j_1}| \star \psi_{j_2}) .$$

These moments measure the average multiscale time variations of $|X \star \psi_{j_1}(t)|$, with a second family of wavelets ψ_{j_2} . If $j_2 < j_1$ then $\overline{S}X(j_1, j_2)$ has a fast decay to zero as $j_1 - j_2$ increases. Its amplitudes depend on the wavelet properties as opposed to the properties of X . Indeed, if $|\psi|$ is \mathbf{C}^p and has p vanishing moments then $|X \star \psi_{j_1}|$ is typically almost everywhere \mathbf{C}^p so

$\overline{S}X(j_1, j_2) = \mathbf{E}(|X \star \psi_{j_1} \star \psi_{j_2}|) = O(2^{p(j_2-j_1)})$. We thus concentrate on scattering moments for $j_2 > j_1$.

The expected value of second order moments averages the time variability of $|X \star \psi_{j_1} \star \psi_{j_2}(t)|$. This lost information can be recovered by calculating the wavelet transform of $|X \star \psi_{j_1} \star \psi_{j_2}(t)|$ for each (j_1, j_2) . Iterating this process computes scattering moments at any order $m \geq 1$:

$$(5) \quad \forall (j_1, \dots, j_m) \in \mathbb{Z}^m, \quad \overline{S}X(j_1, \dots, j_m) = \mathbf{E}(|X \star \psi_{j_1} \star \dots \star \psi_{j_m}|).$$

If $\mathbf{E}(|X(t) - X(t - \tau)|) < \infty$ for all $\tau \in \mathbb{R}$ then $\mathbf{E}(|X \star \psi_{j_1}|) < \infty$ and one can verify by induction on m that $\overline{S}X(j_1, \dots, j_m) < \infty$.

The vector of all scattering moments of X defines a non-parametric representation

$$\overline{S}X = \left\{ \overline{S}X(j_1, \dots, j_m) : \forall (j_1, \dots, j_m) \in \mathbb{Z}^m, \forall m \in \mathbb{N}^* \right\}.$$

Its \mathbf{I}^2 norm is

$$(6) \quad \|\overline{S}X\|^2 = \sum_{m=1}^{\infty} \sum_{(j_1, \dots, j_m) \in \mathbb{Z}^m} |\overline{S}X(j_1, \dots, j_m)|^2.$$

Since the wavelet transform preserves the variance in (4) and the modulus operators obviously also preserves the variance, each wavelet transform and modulus iteration preserves the variance. If $\mathbf{E}(|X|^2) < \infty$ then by applying (4), we verify [22] by induction on l that scattering coefficients satisfy

$$\sum_{m=1}^{l-1} \sum_{(j_1, \dots, j_m) \in \mathbb{Z}^m} |\overline{S}X(j_1, \dots, j_m)|^2 = \sigma^2(X) - \sum_{(j_1, \dots, j_l) \in \mathbb{Z}^l} \mathbf{E}(|X \star \psi_{j_1} \star \dots \star \psi_{j_l}|^2).$$

with $\sigma^2(X) = \mathbf{E}(|X|^2) - |\mathbf{E}(X)|^2$. It results that

$$(7) \quad \|\overline{S}X\|^2 \leq \sigma^2(X).$$

Numerical experiments indicate that for large classes of ergodic stationary processes, $\sum_{(j_1, \dots, j_l) \in \mathbb{Z}^l} \mathbf{E}(|X \star \psi_{j_1} \star \dots \star \psi_{j_l}|^2)$ converges to zero as 2^l increases. It then implies that (7) is an equality. Similarly to the Fourier power spectrum, the \mathbf{I}^2 norm of scattering moments is then equal to the variance. However, this remains a conjecture [22].

The scattering norm (6) can be approximated with a summation restricted to moments of order $m = 1, 2$, because higher order scattering moments usually have a much smaller energy [2, 7]. First and second order scattering

moments applied to image and audio textures as well as intrapartum electrocardiograms for fetal monitoring provide state of the art classification errors [7, 2, 37, 10], but these results are strictly numerical. These algorithms are implemented with deep convolutional neural network structures [21]. In the following, we concentrate on the mathematical properties of first and second order scattering moments, which characterize self-similarity and intermittency properties.

2.3. Normalized Scattering and Intermittency. Scattering moments are normalized to increase their invariance. Invariance to multiplicative factors is obtained with

$$\tilde{S}X(j_1) = \frac{\overline{S}X(j_1)}{\overline{S}X(0)} = \frac{\mathbf{E}(|X \star \psi_{j_1}|)}{\mathbf{E}(|X \star \psi|)}.$$

Second order scattering moments are normalized by their first order moment:

$$\tilde{S}X(j_1, j_2) = \frac{\overline{S}X(j_1, j_2)}{\overline{S}X(j_1)} = \frac{\mathbf{E}(|X \star \psi_{j_1} \star \psi_{j_2}|)}{\mathbf{E}(|X \star \psi_{j_1}|)}.$$

This can be rewritten

$$\tilde{S}X(j_1, j_2) = \overline{S}\tilde{X}_{j_1}(j_2) = \mathbf{E}(|\tilde{X}_{j_1} \star \psi_{j_2}|) \quad \text{with} \quad \tilde{X}_{j_1} = \frac{|X \star \psi_{j_1}|}{\mathbf{E}(|X \star \psi_{j_1}|)}.$$

If X has stationary increments then \tilde{X}_{j_1} is a normalized stationary process providing the occurrence of “burst” of activity at the scale 2^{j_1} . Normalized second order moments $\tilde{S}X(j_1, j_2)$ thus measure the time variability of these burst of activity over time scales $2^{j_2} \geq 2^{j_1}$, which gives multiscale measurements of intermittency.

Intermittency aims at capturing the geometric distribution of burst of high variability in each realization of X . It is not modified by the action of derivative operators, which are translation invariant. We verify that this invariance property holds for normalized second order moments. Let d^α be a fractional derivative defined by the multiplication by $(i\omega)^\alpha$ in the Fourier domain. Since

$$d^\alpha X \star \psi_{j_1}(t) = 2^{-\alpha j_1} X \star \psi_{j_1}^\alpha(t)$$

where $\psi^\alpha = d^\alpha \psi$ and $\psi_{j_1}^\alpha(t) = 2^{-j_1} \psi^\alpha(2^{-j_1} t)$, it results that

$$(8) \quad \overline{S}d^\alpha X(j_1) = 2^{-\alpha j_1} \mathbf{E}(|X \star \psi_{j_1}^\alpha|)$$

and

$$(9) \quad \tilde{S}d^\alpha X(j_1, j_2) = \frac{\mathbf{E}(|X \star \psi_{j_1}^\alpha \star \psi_{j_2}|)}{\mathbf{E}(|X \star \psi_{j_1}^\alpha|)}.$$

If $X(t)$ has no oscillating singularity [17] then its wavelet coefficients calculated with ψ and ψ^α have the same asymptotic decay, so

$$(10) \quad \overline{S}d^\alpha X(j_1) \simeq 2^{-\alpha j_1} \overline{S}X(j_1) \quad \text{and} \quad \widetilde{S}d^\alpha X(j_1, j_2) \simeq \widetilde{S}X(j_1, j_2) .$$

Modifications of regularity produced by derivative operators affect the decay of first-order scattering moments but not the decay of normalized second order moments. Fractional Brownian motions illustrate these properties in Section 3.2.

Global intermittency parameters computed with wavelet moments can be related to normalized second order scattering moments. Section 2.1 explained that multifractal analysis quantifies intermittency from scaling properties of wavelet moments. If $\mathbf{E}(|X \star \psi_j|^q) \simeq 2^{j\zeta q}$ then intermittency is measured by the curvature of $\zeta(q)$. It can be quantified by $\zeta(2) - 2\zeta(1)$ which satisfies

$$\frac{\mathbf{E}(|X \star \psi_j|^2)}{\mathbf{E}(|X \star \psi_j|)^2} \simeq 2^{j(\zeta(2)-2\zeta(1))} .$$

The following proposition relates this ratio to normalized second order scattering moments.

PROPOSITION 2.1. *If X has stationary increments then for any $j_1 \in \mathbb{Z}$*

$$(11) \quad \frac{\mathbf{E}(|X \star \psi_{j_1}|^2)}{\mathbf{E}(|X \star \psi_{j_1}|)^2} \geq 1 + \sum_{j_2=-\infty}^{+\infty} |\widetilde{S}X(j_1, j_2)|^2 .$$

Proof: Applying the mean-square energy conservation (4) to $X \star \psi_j$ proves that

$$(12) \quad \mathbf{E}(|X \star \psi_j|^2) = |\mathbf{E}(|X \star \psi_j|)|^2 + \sum_{j_2=-\infty}^{+\infty} \mathbf{E}(|X \star \psi_j| \star \psi_{j_2}|^2) .$$

Applying again (4) to $||X \star \psi_j| \star \psi_{j_2}|$ proves that

$$\mathbf{E}(|X \star \psi_j| \star \psi_{j_2}|^2) = \mathbf{E}(|X \star \psi_j| \star \psi_{j_2}|)^2 + \sum_{j_3=-\infty}^{+\infty} \mathbf{E}(|X \star \psi_j| \star \psi_{j_2}| \star \psi_{j_3}|^2) .$$

Inserting this equation in (12) proves (11). \square

It results from (12) that if $\sum_{j_2=-\infty}^{+\infty} \widetilde{S}X(j_1, j_2)^2 \simeq 2^{j_1\beta}$ then $\zeta(2) - 2\zeta(1) \geq \beta > 0$. However, these moment computations eliminate the dependence's on the scale parameter 2^{j_2} , which provides a finer multiscale characterization of the intermittency regularity. This dependency upon 2^{j_2} is studied in the next sections and is used for model selection in Section 5.

2.4. *Scattering Poisson Processes.* The properties of scattering moments are illustrated over a Poisson process, which is a simple Lévy process with stationary increments. A homogeneous Poisson process $\{X(t), t \geq 0\}$ has increments $X(t + \Delta) - X(t)$ which count the number of occurrence of events in $[t, t + \Delta]$, and have a Poisson distribution of intensity λ . Figure 1(a) shows an example. The following proposition gives the decay of first and second order scattering moments of Poisson processes.

THEOREM 2.2. *If X is a Poisson process of intensity λ and $\bar{\psi}(t) = \int_0^t \psi(u) du$ then for all $j_1 \leq j_2$*

$$(13) \quad \bar{S}X(j_1) = 2^{j_1} \lambda \|\bar{\psi}\|_1 \left(1 + O(2^{j_1} \lambda)\right),$$

$$(14) \quad \lim_{j_1 \rightarrow \infty} 2^{-j_1/2} \bar{S}X(j_1) = C \lambda^{1/2} > 0,$$

where C depends only upon the wavelet ψ , and

$$(15) \quad \tilde{S}X(j_1, j_2) = \frac{\|\bar{\psi} \star \psi_{j_2-j_1}\|_1}{\|\bar{\psi}\|_1} \left(1 + O(\lambda 2^{j_1}) + O(\lambda 2^{j_2})\right)$$

$$(16) \quad \lim_{j_2 \rightarrow \infty} 2^{j_2/2} \tilde{S}X(j_1, j_2) = C' > 0.$$

The proof is in Appendix A. At scales $2^{j_1} \leq 2^{j_2} \ll \lambda^{-1}$, the Poisson process typically has 1 jump over the support of each wavelet, which implies (13). When $2^{j_1} \gg \lambda^{-1}$, Appendix A proves that $X \star \psi_{j_1}(t)$ converges to the wavelet transform of a Gaussian white noise of variance $\lambda 2^{j_1}$, which implies (14).

When $2^{j_2} \ll \lambda^{-1}$ and $j_2 - j_1$ increases, (15) implies that

$$\lim_{j_1 \rightarrow -\infty} \tilde{S}X(j_1, j_2) = \|\psi\|_1 \left(1 + O(2^{j_2} \lambda)\right).$$

This convergence to a constant indicates a high degree of intermittency, because fine scale wavelets see individual Diracs occurring randomly. This property is observed in Figure 1(d), which gives $\log_2 \tilde{S}X(j_2 - j_1, j_2)$ as a function of $j_2 - j_1$. These curves overlap for different j_1 , and converge to $\|\psi\|_1$.

If $2^{j_2} \gg \lambda^{-1}$ then $\tilde{S}X(j_1, j_2) \simeq 2^{-j_2/2}$. This decay is characteristic of Gaussian stationary processes, which are uniformly regular and thus have no intermittency. This is further studied in Section 3.2 for fractional Brownian

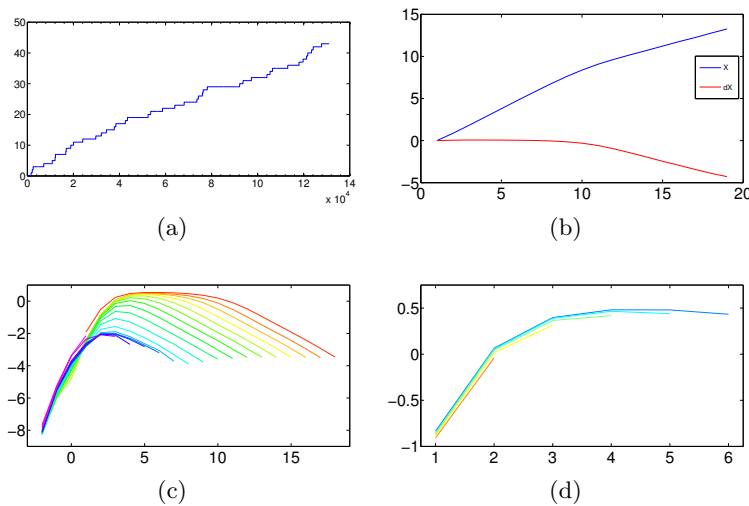


FIG 1. (a): Realization of a Poisson process $X(t)$ of intensity $\lambda = 10^{-4}$. (b): $\log_2 \tilde{S}X(j)$ and $\log_2 \tilde{S}dX(j)$ as a function of j . (c): $\log_2 \tilde{S}X(j_1, j_2)$ as a function of $j_2 - j_1$ for several values of j_1 . (d): The same curves as in (c), but restricted to $j_2 < -\log_2(\lambda) - 1$.

motions. Figure 1(c) verifies that $\tilde{S}X(j_2 - j_1, j_2)$ decays with a slope of $-1/2$ as a function of $j_2 - j_1$.

When going from X to dX then the sum of jumps is replaced by a measure which is a sum of Diracs. We verify from Appendix A that $\overline{S}dX(j_1) \simeq 2^{-j_1} \overline{S}X(j_1)$. This reflects the change of regularity. Figure 1(b) shows that the difference between the slopes of $\log_2 \tilde{S}X(j_1)$ and $\log_2 \tilde{S}dX(j_1)$ is indeed equal to 1. For normalized second order moments, $\tilde{S}dX(j_1, j_2)$ is nearly equal to $\tilde{S}X(j_1, j_2)$. Indeed, dX and X have isolated singularities occurring with same probability distribution, and hence have the same intermittency.

3. Self-Similar Processes. Second order scattering moments of self-similar processes are proved to be stationary across scales. Fractional Brownian motions and Lévy stable processes are studied in Sections 3.2 and 3.3.

3.1. *Scattering Self-Similarity.* Self-similar processes of Hurst exponent H are stochastic processes $X(t)$ which are invariant in distribution under a scaling of space or time:

$$(17) \quad \forall s > 0, \{X(st)\}_t \stackrel{d}{=} \{s^H X(t)\}_t.$$

We consider self-similar processes having stationary increments. Fractional Brownian motions and α -stable Lévy processes are examples of Gaussian

and non-Gaussian self-similar processes with stationary increments.

If X is self-similar, then applying (17) with a change of variable $u' = 2^{-j}u$ in (1) proves that

$$\forall j \in \mathbb{Z} \ , \ \{X \star \psi_j(t)\}_t \stackrel{d}{=} 2^{jH} \{X \star \psi(2^{-j}t)\}_t .$$

The following proposition proves that normalized second order scattering moments can be written as a univariate function.

PROPOSITION 3.1. *If X is a self-similar process with stationary increments then for all $j_1 \in \mathbb{Z}$*

$$(18) \quad \tilde{S}X(j_1) = 2^{j_1 H} \ ,$$

and for all $(j_1, j_2) \in \mathbb{Z}^2$

$$(19) \quad \tilde{S}X(j_1, j_2) = \bar{S}\tilde{X}(j_2 - j_1) \quad \text{with} \quad \tilde{X}(t) = \frac{|X \star \psi(t)|}{\mathbf{E}(|X \star \psi|)} .$$

Proof: We write $L_j x(t) = x(2^{-j}t)$. Since $\psi_{j_1} = 2^{-j_1} L_{j_1} \psi$, a change of variables yields $L_{j_1} |X \star \psi| = |L_{j_1} X \star \psi_{j_1}|$, and hence

$$(20) \quad |X \star \psi_{j_1}| = L_{j_1} |L_{-j_1} X \star \psi| \stackrel{d}{=} 2^{j_1 H} L_{j_1} |X \star \psi| .$$

If $Y(t)$ is stationary then $\mathbf{E}(L_j Y(t)) = \mathbf{E}(Y(t))$, which proves (18).

By cascading (20) we get

$$(21) \quad \forall (j_1, j_2) \ , \ ||X \star \psi_{j_1}| \star \psi_{j_2}| \stackrel{d}{=} 2^{j_1 H} L_{j_1} ||X \star \psi| \star \psi_{j_2 - j_1}| \ ,$$

so $\bar{S}X(j_1, j_2) = 2^{j_1 H} \mathbf{E}(|X \star \psi| \star \psi_{j_2 - j_1})$. Together with (18) it proves (19). \square

Property (19) proves that if X is self-similar then $\tilde{S}X(j_1, j_1 + l)$ is a function of l , which can be interpreted as a stationary property across scales. This function of l is a scattering intermittency measure of the random process. A Brownian motion is a Gaussian self-similar process with a Hurst exponent $H = 1/2$. It results from (18) that $\log_2 \tilde{S}(j_1) = j_1/2$, which is illustrated by Figure 2 (b). Figure 2 (c) displays $\tilde{S}X(j_1, j_2)$ expressed as a function of $j_2 - j_1$, for different j_1 . The curves for different j_1 are equal, as proved by (18). When $j_2 - j_1 < 0$, $\tilde{S}X(j_1, j_2)$ increases with a slope which does not depend on X but on the number of vanishing moments and on the regularity of the wavelet ψ . For $j_2 - j_1 \geq 0$, the decay depends upon the property of X and satisfies $\tilde{S}X(j_1, j_2) \simeq 2^{-(j_2 - j_1)/2}$. Next section proves this result in the more general context of fractional Brownian motions, and shows that it reflects the fact that a Brownian motion is a Gaussian process.

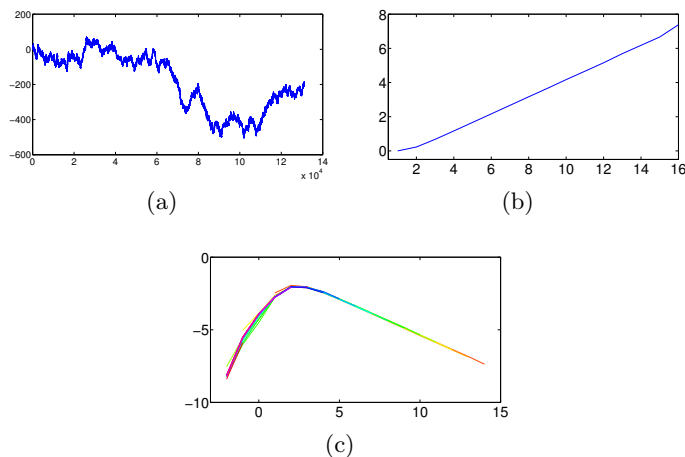


FIG 2. (a): Realization of a Brownian motion $X(t)$. (b): $\log_2 \tilde{S}X(j_1)$ as a function of j_1 . (c) The curves $\log_2 \tilde{S}X(j_1, j_1 + l)$ as a function of l are identical for different j_1 .

3.2. Fractional Brownian Motions. We compute the normalized scattering representation of Fractional Brownian Motions, which are the only self-similar Gaussian processes with stationary increments. A fractional Brownian motion of Hurst exponent $0 < H < 1$ is defined as a zero mean Gaussian process $\{X(t)\}$, satisfying

$$\forall t, s > 0, \mathbf{E}(X(t)X(s)) = \frac{1}{2} (t^{2H} + s^{2H} - |t - s|^{2H}) \mathbf{E}(X(1)^2).$$

It is self-similar and satisfies

$$\forall s > 0, \{X(st)\}_t \stackrel{d}{=} s^H \{X(t)\}_t.$$

Proposition 3.1 proves in (18) that

$$\tilde{S}X(j_1) = 2^{Hj_1}.$$

This is verified by Figure 3(a) which shows that $\log_2 \tilde{S}X(j_1) = H j_1$ for several fractional Brownian motions with $H = 0.2, 0.4, 0.6, 0.8$.

Figure 3(c) displays $\log_2 \tilde{S}(j_1, j_2)$, which is a function of $j_2 - j_1$, as proved by (19). Modulo a proper initialization at $t = 0$, if X is a fractional Brownian motion of exponent H then $d^\alpha X$ is a fractional Brownian motion of exponent $H - \alpha$. We thus expect from (10) that $\log_2 \tilde{S}X(j_2 - j_1)$ nearly does not depend upon H . This is shown by Figure 3(c) where all curve superimpose for $j_2 - j_1 > 0$, with a slope of $-1/2$. This result is proved by the following theorem.

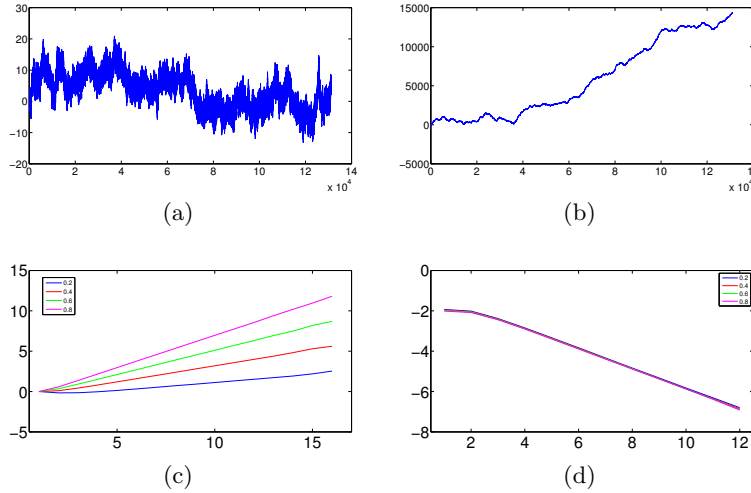


FIG 3. (a,b) Realizations of fractional Brownian motions $X(t)$ with $H = 0.2$ in (a) and $H = 0.8$ in (b). (c) $\log_2 \tilde{S}X(j_1)$ as a function of j_1 , for $H = 0.2, 0.4, 0.6, 0.8$. Slopes are equal to H . (d) $\log_2 \tilde{S}X(j_1, j_1 + l)$ as a function of l do not depend on j_1 for all H .

THEOREM 3.2. *Let $X(t)$ be a Fractional Brownian Motion with Hurst exponent $0 < H < 1$. There exists a constant $C > 0$ such that for all $j_1 \in \mathbb{Z}$*

$$(22) \quad \lim_{l \rightarrow \infty} 2^{l/2} \tilde{S}X(j_1, j_1 + l) = C .$$

Proof: Proposition 3.1 proves in (19) that $\tilde{S}X(j_1, j_1 + j) = \mathbf{E}(|\tilde{X} \star \psi_j|)$ and $\tilde{X}(t) = |X \star \psi(t)| / \mathbf{E}(|X \star \psi|)$. We denote $\tilde{S}_2 X(j) = \mathbf{E}(|\tilde{X} \star \psi_j|)$. Let $B(t)$ be a Brownian motion and $dB(t)$ be the Wiener measure. The two processes $X \star \psi(t)$ and $d^{H-1}dB \star \psi(t)$ are Gaussian stationary processes having same power spectrum so

$$\{|X \star \psi(t)|\}_t \stackrel{d}{=} \{|d^{H-1}dB \star \psi(t)|\}_t \stackrel{d}{=} \{|dB \star d^{H-1}\psi(t)|\}_t .$$

It results that

$$(23) \quad \tilde{S}_2 X(j) = \frac{\mathbf{E}(|dB \star d^{H-1}\psi \star \psi_j|)}{\mathbf{E}(|X \star \psi|)}$$

Since ψ is \mathbf{C}^1 , with a compact support and two vanishing moments, one can verify that $|d^{H-1}\psi(u)| = O((1 + |u|^2)^{-1})$. It results that $|dB \star d^{H-1}\psi|$ is stationary process whose autocorrelation has some decay. As the scale 2^j increases, the second convolution with ψ_j performs a progressively wider averaging. By applying a central-limit theorem for dependent random variables,

the following lemma applied to $\varphi = d^{H-1}\psi$ proves that $2^{j/1}|dB \star d^{H-1}\psi| \star \psi_j$ converges to a Gaussian processes and that its first moment converges to a constant when j goes to ∞ . The theorem result (22) stating that $2^{j/2}\tilde{S}_2X(j)$ converges to a constant results from (23).

LEMMA 3.3. *If $\varphi(u) = O((1 + |u|^2)^{-1})$ then*

$$(24) \quad 2^{j/2}|dB \star \varphi| \star \psi_j(t) \xrightarrow{j \rightarrow \infty} \mathcal{N}(0, \sigma^2 \text{Id}) ,$$

with $\sigma^2 = \|\psi\|_2^2 \int R_Y(\tau) d\tau$ and

$$(25) \quad \lim_{j \rightarrow \infty} \mathbf{E}(|2^{j/2}|dB \star \varphi| \star \psi_j|) = \sigma \sqrt{\frac{\pi}{2}} . \quad \square$$

For a fractional Brownian motion, $\log_2 \tilde{S}X(j_1, j_1 + l)$ do not depend on j_1 or H , and their slopes is thus equal to $-1/2$ when l increases. This value is characteristic of wide-band Gaussian stationary processes. It indicates that there is no intermittency phenomenon at all scales.

3.3. *α -stable Lévy Processes.* In this section, we compute the scattering moments of α -stable Lévy processes and analyze their intermittency behavior for $1 < \alpha \leq 2$. These processes have finite polynomial moments only for degree strictly smaller than $\alpha \leq 2$. The Lévy-Khintchine formula [20] characterizes infinitely divisible distributions from their characteristic exponents. Self-similar Lévy processes have stationary increments with heavy tailed distributions. Their realizations contain rare, large jumps, which are responsible for the blow up of moments larger than α . They induce a strongly intermittency behavior.

For $\alpha > 1$, an α -stable Lévy process $X(t)$ has stationary increments and $\mathbf{E}(|X(t) - X(t - \tau)|) < \infty$ for any $\tau \in \mathbb{R}$. Its scattering moments are thus well defined at all orders. This process satisfies the self-similarity relation

$$(26) \quad \{X(st)\}_t \stackrel{d}{=} s^{\alpha-1} \{X(t)\}_t ,$$

so Proposition 3.1 proves that

$$(27) \quad \tilde{S}X(j_1) = 2^{j_1 \alpha^{-1}} .$$

This is verified in Figure 4 which shows that $\log_2 \tilde{S}X(j_1) = \alpha^{-1} j_1$. First order moments thus do not differentiate a Lévy stable processes from fractional Brownian motions of Hurst exponent $H = \alpha^{-1}$.

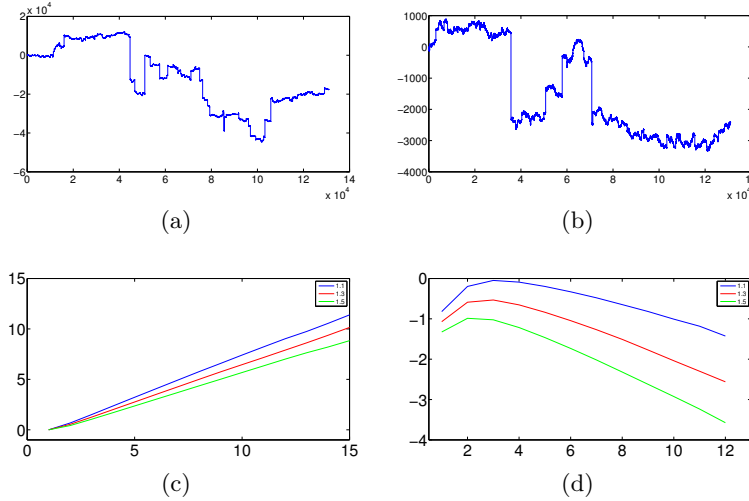


FIG 4. (a,b): Realizations of α -stable Lévy processes $X(t)$ with $\alpha = 1.1$ and $\alpha = 1.5$. (c) $\log_2 \tilde{S}X_\alpha(j_1)$ as a function of j_1 with $\alpha = 1.1, 1.2, 1.3$. Slopes are equal to α^{-1} . (d) $\log_2 \tilde{S}X_\alpha(j_1, j_1 + l)$ as a function of l do not depend on j_1 . Slopes tend to $\alpha^{-1} - 1$ when l increases.

The self-similarity implies that $\tilde{S}X(j_1, j_1 + l)$ does not depend on j_1 . However, they have a very different behavior than second order scattering moments of fractional Brownian motion. Figure 4 shows that $\log_2 \tilde{S}X(j)$ has a slope which tends to $\alpha^{-1} - 1$ and hence that when l increases

$$(28) \quad \tilde{S}X(j_1, j_1 + l) \simeq 2^{l(\alpha^{-1}-1)} .$$

For $\alpha < 2$ then $\alpha^{-1} - 1 > -1/2$ so $\tilde{S}(j_1, j_1 + l)$ has a slower decay for α -stable Lévy processes than for fractional Brownian motion, which corresponds to the fact that these processes are highly intermittent and the intermittency increases when α decreases. For $\alpha = 2$, the Lévy process X is a Brownian motion and we recover that $\tilde{S}X(j_1, j_1 + l) \simeq 2^{-l/2}$ as proved in Theorem 3.2.

The scaling property (28) is explained qualitatively, without formal proof. We proved in (19) that

$$(29) \quad \tilde{S}X(j_1, j_2) = \frac{\mathbf{E}(|X \star \psi(t)| \star \psi_l)}{\mathbf{E}(|X \star \psi|)} \quad \text{for } l = j_2 - j_1.$$

The stationary process $|X \star \psi(t)|$ measures the amplitude of local variations of the process X . It is dominated by a sparse sum of large amplitude bumps of the form $a|\psi(t - u)|$, where a and u are the random amplitudes and

positions of rare large amplitude jumps in $X(t)$, distributed according to the Lévy measure. It results that

$$(30) \quad \mathbf{E}(|X \star \psi| \star \psi_l) \simeq \mathbf{E}(|dX \star |\bar{\psi}| \star \psi_l) \text{ with } \bar{\psi}(t) = \int_0^t \psi(u) du.$$

If $2^l \gg 1$ then $|\bar{\psi}| \star \psi_l \approx \|\bar{\psi}\|_1 \psi_l$, and $\mathbf{E}(|dX \star \psi_l|) \simeq 2^{l(\alpha^{-1}-1)}$ because the Lévy measure $dX(t)$ satisfies the self-similarity property

$$\{dX(st)\}_t \stackrel{d}{=} s^{\alpha^{-1}-1} \{dX(t)\}_t .$$

Inserting (30) in (29) gives the scaling property (28).

4. Scattering Moments of Multiplicative Cascades. We study the scattering representation of multifractal processes which satisfy a stochastic scale invariance property. Section 4.2 studies the particularly important case of log-infinitely divisible multiplicative processes.

4.1. *Stochastic Self-Similar Processes.* We consider processes with stationary increments which satisfy the following stochastic self-similarity:

$$(31) \quad \forall 1 \geq s > 0, \{X(st)\}_{t \leq 2^L} \stackrel{d}{=} A_s \cdot \{X(t)\}_{t \leq 2^L},$$

where A_s is a log-infinitely divisible random variable independent of $X(t)$ and the so-called *integral scale* 2^L is chosen (for simplicity) as a power of 2. The Multifractal Random Measures (MRM) introduced by [31, 6] are important examples of such processes. Let us point out that MRM's are stationary increments versions of grid bound multiplicative cascades initially introduced by Yaglom [41] and Mandelbrot [23, 24], and further studied by Kahane and Peyriere [18]. In that respect, all the results that we obtained on MRM's can be easily generalized to discrete multiplicative cascades. For the sake of conciseness, we did not include them here.

Since X has stationary increments and satisfies (31), with a change of variables, we verify that $\forall j \leq L$, $\{X \star \psi_j(t)\}_t \stackrel{d}{=} A_{2^j} \{X \star \psi(2^{-j}t)\}_t$, and hence, for all $q \in \mathbb{Z}$ and $j \leq L$

$$(32) \quad \mathbf{E}(|X \star \psi_j|^q) = \mathbf{E}(|A_{2^j}|^q) \mathbf{E}\{|X \star \psi|^q\} \simeq C_q 2^{j\zeta(q)},$$

where $\zeta(q)$ is a priori a non-linear concave function of q [15]. Similarly to Proposition 3.1, the following proposition shows that normalized scattering moments capture stochastic self-similarity with a univariate function.

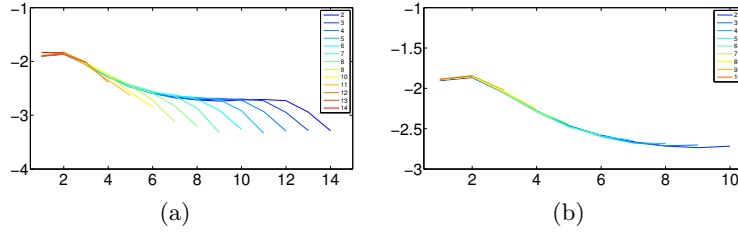


FIG 5. (a): $\log_2 \bar{S}X_\alpha(j_1, j_1 + l)$ as a function of l for a Multifractal Random Measure (MRM) with $\lambda^2 = 0.04$ and an integral scale $2^L = 2^{13}$. Different colors stand for different values of j_1 . (b): Same curves restricted to $j_2 = j_1 + l < L - 1$.

PROPOSITION 4.1. *If X is randomly self-similar in the sense of (31) with stationary increments then for all $j_1 \leq L$*

$$(33) \quad \tilde{S}X(j_1) = \mathbf{E}(|A_{2^{j_1}}|).$$

Moreover, if $2^{j_1} + 2^{j_2} \leq L$ then

$$(34) \quad \tilde{S}X(j_1, j_2) = \bar{S}\tilde{X}(j_2 - j_1) \quad \text{with} \quad \tilde{X}(t) = \frac{|X \star \psi(t)|}{\mathbf{E}(|X \star \psi|)}.$$

Proof: Property (18) is a particular case of (32) for $q = 1$. If $j_1 + j_2 \leq L$, with the same derivations as for (21), we derive from (31) that

$$(35) \quad ||X \star \psi_{j_1}| \star \psi_{j_2}| \stackrel{d}{=} A_{2^{j_1}} L_{j_1} |X \star \psi| \star \psi_{j_2 - j_1}|,$$

so $\bar{S}X(j_1, j_2) = \mathbf{E}(A_{2^{j_1}}) \mathbf{E}(|X \star \psi| \star \psi_{j_2 - j_1}|)$. Together with (33) it proves (34). \square .

Figure 5 shows the normalized scattering of a multiplicative cascade process described in Section 4.2, with an integral scale $2^L = 2^{17}$. When $2^{j_2} \geq 2^L$ is beyond the integral scale, as for a Poisson process, wavelet coefficients converge to Gaussian processes. It results that $\log_2 \tilde{S}(j_1, j_2)$ decays with a slope $-1/2$ as a function of $j_2 - j_1$ for $j_2 > L$, as shown in Figure 5(a). If $j_1 < j_2 < L$ then (34) proves that $\tilde{S}X(j_1, j_2)$ only depends on $j_2 - j_1$, and all curves in Figure 5(b) superimpose in this range.

Propositions 3.1 and 4.1 show that the stationary property $\tilde{S}X(j_1, j_2) = \tilde{S}X(j_2 - j_1)$ can be used to detect the presence of self-similarity, both deterministic and stochastic. This necessary condition is an alternative to the scaling of the q -order moments, $\mathbf{E}(|X \star \psi_j|^q) \simeq C_q 2^{j\zeta(q)}$, which is difficult to verify empirically for $q \geq 2$ or $q < 0$.

4.2. *Log-infinitely divisible Multifractal Random Processes.* Multiplicative cascades as introduced by Mandelbrot in [23, 24] are built as an iterative process starting at scale 2^L . They are obtained as the (weak) limit of the measure dM_n whose restriction over a dyadic interval of the form $[k2^{L-n}, (k+1)2^{L-n}]$ is uniform and equal to $\prod_{i=1}^n W_i^{(k)} dt$, where the $W_i^{(k)}$'s are iid log-infinitely divisible random variables. Multifractal Random Measures (MRM), introduced in [31, 6], can be seen as stationary increments versions of these multiplicative cascades. They are built using an infinitely divisible random noise dP distributed in the half-plane (t, s) ($s > 0$). Using the previous notations, the noise around (t, s) can be seen as the equivalent of the infinitely divisible variable $\log_2 W_{\log s}^{(t/s)}$. More precisely, if $\omega_l^{2^L}(t) = \int_{\mathcal{A}_l^{2^L}(t)} dP$ where $\mathcal{A}_l^{2^L}(t)$ is the cone in the (t, s) half-plane pointing to point $(t, 0)$ and truncated for $s < l$, the MRM is defined as the weak limit: $dM(t) = \lim_{l \rightarrow 0} e^{\omega_l^{2^L}(t)} dt$. For a rigorous definition of $\omega_l^{2^L}$ and of a Multifractal Random Measure, we refer the reader to [6].

One can prove that dM is a stochastic self-similar process in the sense of (31). It is multifractal in the sense that

$$\mathbf{E}(|X \star \psi_j|^q) = \mathbf{E}(|A_{2^j}|^q) \mathbf{E}\{|X \star \psi|^q\} \simeq C_q 2^{j\zeta(q)},$$

where $\zeta(q)$ is a non-linear function which is uniquely defined by the infinitely divisible law chosen for dP . If dP is Gaussian, dM is generally referred to as a "log-Normal" MRM, and in this case [6]:

$$(36) \quad \zeta(q) = \left(1 + \frac{\lambda^2}{2}\right)q - \frac{\lambda^2}{2}q^2.$$

The curvature of the concave function $\zeta(q)$ at $q = 0$ (λ^2 in the latter case) plays the role of the so-called "intermittency factor" in the multifractal formalism [15]. The larger λ^2 , the more intermittency.

The self-similarity properties of dM are mainly direct consequences of the "global" self-similarity properties of $\omega_l^{2^L}$:

$$(37) \quad \{\omega_{sl}^{s2^L}(st)\}_t \stackrel{law}{=} \{\omega_l^{2^L}(t)\}_t, \quad \forall L, \forall s > 0,$$

and of the stochastic self-similarity property :

$$(38) \quad \{\omega_{sl}^{2^L}(su)\}_{u < T} \stackrel{law}{=} \{\Omega_s + \omega_l^{2^L}(u)\}_{u < T}, \quad \forall L, \forall s < 1$$

where Ω_s is an infinitely divisible random variable independent of $\omega_l^{2^L}(u)$ such that $E(e^{q\Omega_s}) = e^{-(q-\zeta(q))\ln(s)}$. More precise results used in the proofs are stated in Appendix C.

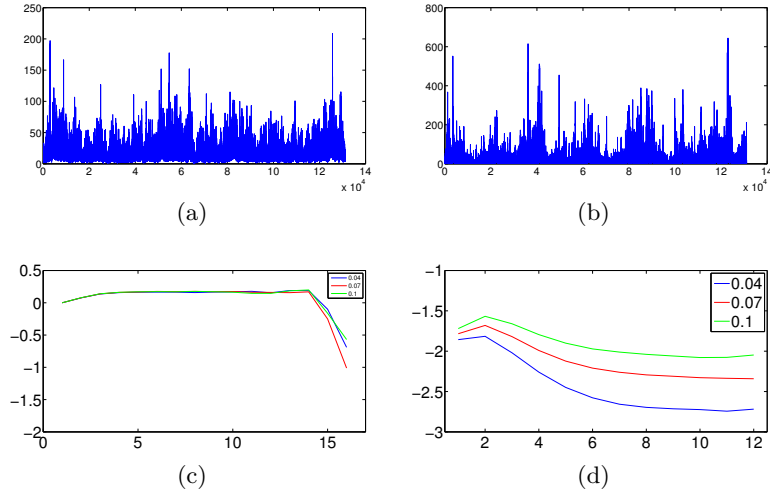


FIG 6. (a,b) Realizations dM of log-normal Multifractal Random Measures with $\lambda^2 = 0.04$ and $\lambda^2 = 0.1$. (c) $\log_2 \tilde{S}dM(j_1)$ with $\lambda^2 = 0.04$, $\lambda^2 = 0.07$ and $\lambda^2 = 0.1$. (d) $\log_2 \tilde{S}dM(j_1, j_1 + l)$, for $\lambda^2 = 0.04$, $\lambda^2 = 0.07$ and $\lambda^2 = 0.1$, as a function of l , for $j_1 + l < L$ where $2^L = 2^{13}$ is the integral scale.

In this section, we will study the scaling properties of scattering moments associated with $X = dM$. Thanks to the discussion in Section 2.3, one can easily show that all our results can be extended to $X(t) = M(t) = \int_0^t dM$. The following theorem characterizes the behavior of normalized first and second order scattering moments of dM :

THEOREM 4.2. *Let dM be a Multifractal Random Measure, then:*

$$(39) \quad \forall j < L, \quad \tilde{S}dM(j) = 1,$$

and if $\zeta(2) > 1$ then as long as $j_1, j_2 < L$, $\tilde{S}dM(j_1, j_2)$ depends only on $j_1 - j_2$ and there exists $\tilde{K} > 0$ such that for each $j_2 \leq L$

$$(40) \quad \lim_{j_1 \rightarrow -\infty} \tilde{S}dM(j_1, j_2) = \tilde{K}.$$

The proof is in Appendix D. Let us illustrate this Theorem in the log-normal case. Figures 6(a,b) displays two realizations of log-Normal MRM cascades for $\lambda^2 = 0.04$ and $\lambda^2 = 0.07$, with an integral scale $2^L = 2^{13}$. Figure 6(c) shows estimations of normalized first order scattering moments for $\lambda^2 = 0.04$, $\lambda^2 = 0.07$ and $\lambda^2 = 0.1$. As predicted by Theorem 4.2, $\log_2 \tilde{S}dM(j_1) = 0$ for $j_1 < L = 13$. The second order scattering moments for

the same values of λ^2 are displayed in Figure 6(d). As expected from Theorem 4.2, $\log_2 \tilde{S}dM(j_1, j_2)$ only depends on $j_2 - j_1$ for $j_2 < L$. It converges to a constant \tilde{K} when $j_2 - j_1$ increases.

With a Taylor expansion, one can show that, for large $j_2 - j_1$, \tilde{K} is a linear function of λ up to some $O(\lambda^2)$ additive term. This is numerically verified by Monte Carlo simulations which shows that $\tilde{K} \approx 0.82\lambda$. We see here again the correspondence between scattering coefficients and intermittency measurements. The constant 0.82 depends upon the choice of wavelet ψ .

Another important class of stochastic self-similar processes is obtained by performing a change of variable in a Brownian motion $B(t)$ with an MRM $M(t)$. The so-obtained process $X(t) = B(M(t))$ is referred to as a Multifractal Random Walks (MRW)[30, 6] and can be obtained as the limit when l goes to 0 of

$$(41) \quad X_l(t) = l^{\frac{2-\zeta(2)}{2}} \int_0^t e^{\omega_l^{2L}(u)} dB(u) ,$$

where $dB(u)$ is the standard Wiener noise. Accordingly, $B(M(t))$ can be considered as a stochastic volatility model, where the associated MRM,

$$(42) \quad \frac{dM_l(u)}{du} = l^{2-\zeta(2)} e^{2\omega_l^{2L}(u)}$$

corresponds to the local stochastic variance. In that respect, such a model can account for asset price fluctuations in financial markets by mimicking the stochastic behavior of asset volatility [30, 4, 5].

Since $B(t)$ is self-similar, one can verify that $X(t)$ inherits the stochastic self-similarity of $M(t)$ and satisfies (32). In particular, one can show (see e.g. [6]) that the multifractal spectrum $\zeta(q)$ of the MRW $X(t)$ defined in (41) is related to the spectrum $\zeta_M(q)$ of the MRM $M(t)$ defined in (42) through:

$$(43) \quad \zeta(q) = \zeta_M(q/2) .$$

Another consequence is that scattering moments of a multifractal random walk behave similarly as the scattering moments of dM . The analog for MRW of the theorem 4.2 along with some numerical illustrations are provided in Appendix E.

5. Parametric Model Estimation with Scattering Moments. Section 5.1 introduces estimators of scattering moments. Section 5.2 applies the generalized method of simulated moments to scattering moments to estimate the parameters of data generating models. Section 5.5 and 5.6 analyze the scattering moments of turbulence data and financial time series to evaluate fractional Brownian, Lévy stable and multifractal cascade models. Computations are performed with a Selesnik compactly supported wavelet [36].

5.1. *Estimation of Scattering Moments.* We study scattering moment estimators introduced in [22], and compute upper bounds of their mean-square error. A scattering moment $\bar{S}X(j_1, \dots, j_m) = \mathbf{E}(|X \star \psi_{j_1} | \star \dots \star \psi_{j_m}|)$ is estimated by replacing the expected value by a time averaging at a scale 2^M . It is calculated with a time window $\phi_M(t) = 2^{-M} \phi(2^{-M}t)$ with $\int \phi(t) dt = 1$. For any $(j_1, \dots, j_m) \in \mathbb{Z}^m$ with $j_k \leq M$, the estimator is

$$(44) \quad \widehat{S}X(j_1, \dots, j_m) = |X \star \psi_{j_1} | \star \dots \star \psi_{j_m}| \star \phi_M(t_0) ,$$

where t_0 is typically in the middle of the domain where $X(t)$ is known. Since $\int \phi_M(t) dt = 1$, this estimator is unbiased $\mathbf{E}(\widehat{S}X(j_1, \dots, j_m)) = \bar{S}X(j_1, \dots, j_m)$. The following theorem, proved in Appendix F, gives an upper bound of the mean squared estimation error at each scale:

THEOREM 5.1. *Suppose that the Fourier transform $\Phi(\omega)$ of ϕ satisfies*

$$(45) \quad |\Phi(\omega)|^2 \leq \frac{1}{2} \sum_{j=1}^{\infty} (|\Psi(2^j \omega)|^2 + |\Psi(-2^j \omega)|^2) \text{ with } \Phi(0) = 1 .$$

If X has stationary increments and $\mathbf{E}(|X \star \psi_{j_1}|^2) < \infty$ then the mean squared estimation error

$$\epsilon(j_1) \stackrel{\text{def}}{=} \mathbf{E}(|\widehat{S}X(j_1) - \bar{S}X(j_1)|^2) + \sum_{m=2}^{\infty} \sum_{-\infty < j_2, \dots, j_m \leq M} \mathbf{E}(|\widehat{S}X(j_1, \dots, j_m) - \bar{S}X(j_1, \dots, j_m)|^2)$$

satisfies

$$(46) \quad \epsilon(j_1) \leq \sigma^2(|X \star \psi_{j_1}|) - \sum_{m=2}^{\infty} \sum_{-\infty < j_2, \dots, j_m \leq M} |\bar{S}X(j_1, \dots, j_m)|^2 .$$

When j_1 is close to M then $|X \star \psi_{j_1}(t)|$ decorrelates slowly relatively to the averaging window scale 2^M so $\epsilon(j_1)$ is large, but it is bounded by $\sigma^2(|X \star \psi_{j_1}|)$. Large variance estimators $\widehat{S}X(j_1, \dots, j_m)$ are eliminated by keeping only small scales $j_k \leq J$ for $1 \leq k \leq m$, with $M - J$ sufficiently large. For most classes of random processes, including fractional Brownian motions and multifractal random walks, we observe numerically that $\epsilon(j_1)$ converges to zero as the averaging scale 2^M goes to ∞ . Equation (46) proves that it is the case if for all j_1

$$\sigma^2(|X \star \psi_{j_1}|) = \sum_{m=2}^{\infty} \sum_{-\infty < j_2, \dots, j_m \leq \infty} |\bar{S}X(j_1, \dots, j_m)|^2 .$$

This energy conservation has been conjectured for large classes of processes in [22], but it is not proved.

For n independent realizations $\{X_k(t)\}_{1 \leq k \leq n}$, we compute an averaged scattering estimator

$$(47) \quad \widehat{S}X = n^{-1} \sum_{k=1}^n \widehat{S}X_k .$$

Its variance is thus reduced by n^{-1} . When n goes to ∞ , the central limit theorem proves that $\widehat{S}X - \overline{S}X$ converges to a zero-mean normal distribution whose variance goes to 0.

5.2. *Generalized Method of Simulated Scattering Moments.* The generalized method of simulated moments [?] computes parameter estimators for data generative models, from arbitrary families of moments. We apply it to scattering moments.

Suppose that $\{X_k\}_{1 \leq k \leq n}$ are n independent realizations of a parametric model Y_θ . Then $\widehat{S}X_k$ is an unbiased estimator of $\overline{S}Y_\theta$ so $m(\theta) = \mathbf{E}(\widehat{S}X_k) - \overline{S}Y_\theta = 0$. The generalized method of moments estimates this moment condition by an empirical average defined by

$$(48) \quad \widehat{m}(\theta) = n^{-1} \sum_{k=1}^n \widehat{S}X_k - \overline{S}Y_\theta = \widehat{S}X - \overline{S}Y_\theta .$$

When n goes to ∞ the central limit theorem proves that $\widehat{m}(\theta)$ converges to a normal distribution. The generalized method of moments finds the parameter $\widehat{\theta}$ such that:

$$(49) \quad \widehat{\theta} = \underset{\theta}{\operatorname{argmin}} \widehat{m}(\theta) W \widehat{m}(\theta)^T$$

for appropriate matrices W . Setting $W = Id$ gives

$$(50) \quad \widehat{\theta}_1 = \underset{\theta}{\operatorname{argmin}} \|\widehat{S}X - \overline{S}Y_\theta\|^2 .$$

The two-step generalized method of moment updates the first estimator $\widehat{\theta}_1$ by setting $W = \widehat{W}_{\widehat{\theta}_1}$, where \widehat{W}_θ is the inverse of the empirical covariance

$$(51) \quad \widehat{W}_\theta = \left(n^{-1} \sum_{k=1}^n (\widehat{S}X_k - \overline{S}Y_\theta)(\widehat{S}X_k - \overline{S}Y_\theta)^T \right)^{-1} .$$

It computes

$$(52) \quad \hat{\theta} = \underset{\theta}{\operatorname{argmin}} \widehat{m}(\theta) \widehat{W}_{\hat{\theta}_1} \widehat{m}(\theta)^T .$$

Since in general we can not compute \overline{SY}_θ analytically, according to the simulated method of moments [26], \overline{SY}_θ is replaced in (48) and (51) by an estimator \widehat{SY}_θ calculated with a Monte Carlo simulation. This estimator is computed with $n' \gg n$ realizations which are adjusted in order to yield a negligible mean-square error $\mathbf{E}(\|\widehat{SY}_\theta - \overline{SY}_\theta\|^2)$. We also compute a p-value for the null hypothesis which supposes that the parametrized model is valid. The J -test [14] is a chi-squared goodness of fit test normalized by the $p - d$ degrees of freedom:

$$(53) \quad \chi_{\text{red}}^2 = (p - d)^{-1} n \widehat{m}(\hat{\theta}) \widehat{W}_{\hat{\theta}} \widehat{m}(\hat{\theta})^T .$$

Under the null hypothesis, $(p - d)\chi_{\text{red}}^2$ asymptotically follows a chi-squared distribution with $p - d$ degrees of freedom.

In practical applications, one must optimize the number p of scattering moments to have enough discriminability with an estimator having small variance. In the present work, we limit ourselves to first and second order scattering. We often need to eliminate the finest scale coefficients $j_1 \leq J_0$ to remove high frequency errors due to aliasing, discretization or to some data smoothing. As explained in Section 5.1, we only keep coefficients below a maximum scale $j_1 \leq J$ and $j_2 \leq J$, to eliminate the largest variance scattering estimators. As explained in Section 2.2, second order moments $\overline{SX}(j_1, j_2)$ for $j_2 \leq j_1$ are also eliminated because they carry little information on X . The resulting scattering vector is thus

$$\overline{SX} = \left(\overline{SX}(j_1), \overline{SX}(j_1, j_2) \right)_{J_0 < j_1 \leq J, j_1 < j_2 \leq J} .$$

It has $J - J_0$ first order scattering moments and $(J - J_0 - 1)(J - J_0)/2$ second order moments.

The Generalized Method of Simulated Moments can also be applied if we observe a single realization $X(t)$ where sufficiently far away wavelet coefficients become independent, since this guarantees that \widehat{SX} becomes asymptotically normal. Let us consider scattering vector estimators computed at intervals Δ :

$$(54) \quad \widehat{SX}_k(j_1) = |X \star \psi_{j_1}| \star \phi_M(k\Delta) \quad \text{and} \quad \widehat{SX}_k(j_1, j_2) = ||X \star \psi_{j_1}| \star \psi_{j_2}| \star \phi_M(k\Delta) .$$

The goodness of fit J-test supposes that the variable (53) follows a chi-squared distribution with $p - d$ degrees of freedom, which requires that

the estimators $\widehat{S}X_k$ are independent for different k . If X has an integral scale T , as in multifractal cascades, then increments are independent at distances larger than T . One can thus set $\Delta = 2T$. Other processes, such as fractional Brownian motions have no integral scales but their wavelet coefficients become nearly independent at distances much larger than the scale. Nearly independent estimators are thus obtained if $\Delta \gg 2^M$.

The situation is easier if we are only interested in the parameter estimator $\widehat{\theta}$ with (52) without goodness of fit. Its consistency requires that $\widehat{S}X$ converges to a normal distribution, but we can estimate its covariance up to an unknown multiplicative factor. It is then unnecessary to estimate the decorrelation properties of wavelet coefficients, and one can set $\Delta = 1$ to be the process sampling interval. It introduces a multiplicative factor in the covariance estimation, which does not affect the estimator $\widehat{\theta}$ in (52).

5.3. Intermittency Estimation on Multiplicative Cascades. The properties of the Scattering Method of Moments are illustrated on the estimation of the intermittency parameter $\theta = \lambda^2$ for multifractal random measures. Section 4.2 proves that normalized second order scattering moments converge to a constant \widetilde{K} which is proportional to λ , showing that the intermittency λ^2 is characterized by first and second order scattering moments. However, the information is not just carried by this asymptotic value, which is why all scattering moments are used for the estimation. The scattering estimation is compared with two estimators dedicated to this particular estimation problem [5].

Scattering moment estimators are computed from n independent realizations of size 2^{11} of a multifractal random measure having an integral scale $T = 2^{10}$. The total number of data points is $N = n \cdot 2^{11}$, and we set $J_0 = 0$. For different values of $N = n \cdot 2^{11}$, we report in Table 1 the value of J which minimizes the mean squared error $\mathbf{E}(|\widehat{\theta} - \theta|^2)$, estimated with Monte Carlo simulations. We also give the average value of the reduced χ_{red}^2 test in (53) and the model p-value. For small values of n , the covariance of $\widehat{S}X$ is computed up to a multiplicative constant, from correlated scattering coefficients calculated within each realization with $\Delta = 1$ in (54). It leads to a good estimation of $\widehat{\theta}$ but the model p-value can not be estimated.

The intermittency parameter of multifractal random measures can also be estimated directly from wavelet coefficients. Section 4.2 explains that the scaling exponent of wavelet moments of order q is $\zeta(q) = (\frac{1}{2} + \lambda^2)q - \frac{\lambda^2}{2}q^2$. It results that $\lambda^2 = 2\zeta(1) - \zeta(2)$. The intermittency parameter can thus be estimated with a linear regression on the estimated first and second order

TABLE 1

Estimation of λ^2 for a multifractal random measure. The table gives the mean and the standard deviation of estimators computed with a wavelet moment regressions (55), a log covariance regression (56), and the method of simulated scattering moments, for several values of λ^2 and several sample sizes $N = n \cdot 2^{11}$.

λ^2	N	$\widehat{\theta}$ Wavelet	$\widehat{\theta}$ log-cov	$\widehat{\theta}$ Scattering	J	χ_{red}^2	p-value
0.02	10^6	$0.025 \pm 2 \cdot 10^{-3}$	$0.02 \pm 2 \cdot 10^{-4}$	$0.02 \pm 2 \cdot 10^{-4}$	7	1.1 ± 0.3	0.7 ± 0.3
0.05	10^6	$0.055 \pm 2 \cdot 10^{-3}$	$0.05 \pm 6 \cdot 10^{-4}$	$0.05 \pm 3 \cdot 10^{-4}$	6	0.8 ± 0.3	0.5 ± 0.3
0.1	10^6	$0.105 \pm 4 \cdot 10^{-3}$	0.1 ± 10^{-3}	0.1 ± 10^{-3}	5	0.8 ± 0.5	0.5 ± 0.3
0.1	10^5	0.109 ± 10^{-2}	$0.1 \pm 3 \cdot 10^{-3}$	$0.1 \pm 2 \cdot 10^{-3}$	5	0.7 ± 0.3	0.3 ± 0.3
0.1	10^4	$0.12 \pm 3 \cdot 10^{-2}$	$0.1 \pm 1.3 \cdot 10^{-2}$	$0.1 \pm 9 \cdot 10^{-3}$	5	N/A	N/A

moments of wavelet coefficients at scales $2^j < 2^L$:

$$(55) \quad 2 \log_2 \mathbf{E}(|X \star \psi_j|^2) - \log_2 \mathbf{E}(|X \star \psi_j|)^2 \approx j(\zeta(2) - 2\zeta(1)) + C .$$

The wavelet moments $\mathbf{E}(|X \star \psi_j|^2)$ and $\mathbf{E}(|X \star \psi_j|)$ are estimated with empirical averages of $|X \star \psi_j|$ and $|X \star \psi_j|^2$, calculated from the N data samples. An improved estimator has been introduced in [4, 5] with a regression on the covariance of the log of the multifractal random measure. One can indeed prove that

$$(56) \quad \text{Cov}(\log |X \star \psi_j(t)|, \log |X \star \psi_j(t+l)|) \simeq -\lambda^2 \ln \left(\frac{l}{2^L} \right) + o \left(\frac{j}{l} \right) ,$$

which leads to lower variance estimations.

Table 1 shows that the scattering moment estimation of λ^2 has a smaller variance than the regression of first and second order wavelet moments. This is due to the low variance of the scattering estimators which are computed with non-expansive operators. It gives comparable results with the log-covariance estimator, which was optimized for this problem [5]. The J-test validates the multifractal model, since we obtain a normalized J-test with mean and standard deviation close to $1 \pm \sqrt{\frac{2}{p-1}}$, corresponding to mean and standard deviation of a chi-squared distribution with $p - 1$ degrees of freedom. The resulting p-values for rejecting the true model are of the order of 0.5. As expected, reducing the maximum scattering scale J improves the estimation of λ^2 for high intermittences. It removes large variance coefficients. However, numerical experiments confirm that the generalized method of moments is robust to the choice of J , because the inverse covariance \widehat{W} in (52) reduces the impact of high variance coefficients.

TABLE 2

Estimation of α for α -stable Lévy. The table gives the mean and the standard deviation of estimators computed with a wavelet moment regressions (55) and the method of simulated scattering moments, for several values of α for $N = n \cdot 2^{11}$.

α	$\hat{\theta}$ Wavelet	$\hat{\theta}$ Scattering	J
1.1	?	$1.1 \pm 8 \cdot 10^{-3}$	7
1.5	?	?	6

5.4. *Estimation of Blumenthal-Gethoor Index on Lévy Processes.* We apply the same methodology to estimate the Blumenthal-Gethoor index of Lévy processes, defined as

$$\beta = \inf \left\{ r \geq 0 \text{ s.t. } \int_{|x| \leq 1} |x|^r d\Pi(x) < \infty \right\},$$

where $\Pi(x)$ is the Lévy measure associated to an observed Lévy process $X(t)$. If $X(t)$ is α -stable, then $\beta = \alpha$. This index can be estimated using spectral methods in [?], which require an estimation of the characteristic function.

We concentrate in the case of α -stable processes, and we assume here that $1 < \alpha \leq 2$, which implies that we cannot consider the covariance of $\widehat{S}X$. Instead, we use the simplified GMM estimator (50).

- Missing: Lévy with 1.5.
- Compare with wavelet regression. (1st order)
- Competing method?

5.5. *Turbulence Energy Dissipation.* Turbulent regimes that appear in a wide variety of experimental situations, are characterized by random fluctuations over a wide range of time and space scales. Making a theory of the famous Richardson “energy cascade” across the inertial range remains one of the main challenges in classical physics [13]. Normalized scattering moments are computed over dissipative measurements of a turbulent gas, to analyze their self-similarity and intermittency properties. The precision of fractional Brownian motion, Lévy stable and multifractal random measure models are evaluated with a J-test resulting from scattering moments. This study does not pretend evaluating general turbulence physical models. However, it shows that one can have confident model evaluations from data sets, despite intermittency phenomena.

The data we used have been recorded by the group of B. Castaing in Grenoble in a low temperature gaseous Helium jet in which the Taylor scale

based Reynolds number is $R_\lambda = 703$ [9]. A single probe provides measures of velocity temporal variations at a fixed space location that involve both Lagrangian and Eulerian fluctuations. Figure 7-(a) shows a sample of the surrogate dissipation field $X(t)$ as a function of time, estimated from the experimental velocity records ¹. The Kolmogorov (dissipative) scale η is observed at approximately 2^2 sample points, whereas the integral scale is approximately $2^L = 2^{11}$ sample points.

First order scattering coefficients are normalized at the finest scale defined by $j_1 = 2$. These coefficients are displayed in Figure 7(b). In the inertial range $2^1 = 2^{j_0} < 2^{j_1} \leq 2^L = 2^{11}$ the scaling law of the exponents is $\tilde{S}X(j_1) \simeq 2^{-0.25j_1}$. If $2^{j_1} \geq 2^L$ then $\tilde{S}X(j_1) \simeq 2^{-j_1/2}$ because the low frequencies of a turbulent flow becomes Gaussian and independent beyond the integral scale.

Figure 7(c) gives estimated normalized second order coefficients $\log_2 \tilde{S}X(j_1, j_1 + l)$ as a function of l , for different j_1 . For $j_2 = j_1 + l > L$, the slopes increase up to $-1/2$ because beyond the integral scale, wavelet coefficients converge to Gaussian random processes. Below the integral scale, $j_2 = j_1 + l < L - 1$ Figure 7(d) shows the curves $\log_2 \tilde{S}X(j_1, j_1 + l)$ with error bars giving the standard deviations of each estimated values. In this inertial range, the average slope of all curves is -0.2 . This slope is very different from the $-1/2$ decay of Gaussian processes, which indicate the presence of intermittent phenomena. Although these curves are similar, one can observe that they differ significantly compared to the error bars, which indicates the self-similarity of turbulence data is violated. This non-self-similarity is likely to originate from the fact that, as already observed in [12, 8], Taylor hypothesis does not rigorously hold.

We consider the three following models for inertial range turbulence : (i) the square of a Fractional Gaussian Noise parametrized by $\theta = H$, (ii) the square of the increments of α -stable Lévy processes, parametrized by $\theta = \alpha$, and finally (iii) log-normal multifractal random measures, parametrized by the intermittency parameter $\theta = \lambda^2$. Setting $J_0 = 1$ eliminates coefficients below the diffusion scale. We have $N = 4 \cdot 10^6$ data samples, divided into 4 realizations. Within each realization, since the integral scale is $T = 2 \cdot 10^3$, samples are independent at a distance larger than T . The maximum scale is set to $2^J = 2^8$ but its modification has a marginal impact on the estimation. The size of the resulting scattering vector is $p = (J - J_0 + 1)(J - J_0)/2 = 28$.

Table 3 gives an optimal parameter $\hat{\theta}$ as well as the value of the χ_{red}^2 goodness of fit test in (53), together with its p-value. All models are rejected with very high confidence. For nearly the same number of data val-

¹One assumes the validity of the Taylor hypothesis [13]

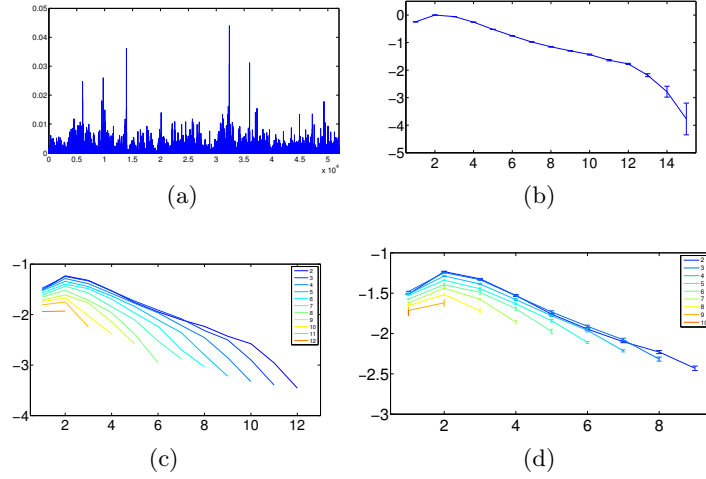


FIG 7. (a) Realization of dissipation $X(t) = \left(\frac{\partial v}{\partial t}\right)^2$ in a turbulent flow. (b) Estimation $\log_2 \widehat{S}X(j_1)$ as a function of j_1 , calculated from 4 realizations of 2^{19} samples each. (c) $\log_2 \widehat{S}X(j_1, j_1+l)$ as a function of l , for $2 \leq j_1 \leq 12$. (d) $\log_2 \widehat{S}X(j_1, j_1+l)$ in the inertial range $j_1+l < L-1 = 10$. We plot the confidence intervals corresponding to the standard deviation of the estimated $\log_2 \widehat{S}X(j_1, j_1+l)$.

TABLE 3

Parameter estimation for the turbulence data in Figure 7(a), calculated from Fractional Brownian Noise measures (FBN), Lévy stable measures (LS), and Multifractal Random Measures (MRM).

	FBN	LS	MRM
$\hat{\theta}$	$H = 0.9$	$\alpha = 1.98$	$\lambda^2 = 0.09$
χ^2_{red}	28	29	29
p-value	$< 10^{-6}$	$< 10^{-6}$	$< 10^{-6}$

ues, with integral scales of same size, Table 1 gave much higher p-values for valid multifractal random measure models of same intermittency. The main source of errors of each model clearly appears by analyzing the normalized scattering moments in Figure 7. Fractional Brownian motions have first order coefficients which can mimic the decay of the first order scattering coefficients but not the one of their second order coefficients ($-1/2$ as opposed to -0.2). Lévy stable processes have first and second order scattering coefficients which decay with a slope of $\alpha^{-1} - 1$. To match the slopes in Figure 7(c,d), respectively equal to -0.25 and -0.2 , we would need that $\alpha \approx 1.2$ which is far from the value $\alpha = 1.98$ obtained in Table 3. Multifractal random measure model misfit comes from their first order coefficients which remain constant whereas turbulence data coefficients decay with a slope close to -0.2 .

5.6. Financial Time-Series Analysis. In the following, we analyze the normalized scattering moments of two financial time series: high-frequency Euro-Bund trade data ² and intraday S&P 100 index trade data. Each trade occurs at a given price, whose logarithm is noted $X(t)$.

Every single day, the logarithmic returns of the price (i.e., the increments of $X(t)$) are computed on rolling 10 second intervals, after preprocessing the microstructure noise using the technique advocated in [34]. Each day corresponds to 9 hours of trading and hence 3240 increments. Intraday financial data are subject to strong seasonal intraday effects. These effects are removed with a standard “deseasonalizing” algorithm which normalizes the returns by the square root of the intraday seasonal variance.

Figure 8(a) shows the resulting “deseasonalized” Euro-Bund log-price $X(t)$ for a particular day. Figure 8(b) shows $\log_2 \tilde{S}X(j_1)$ as a function of j_1 . The slope is 0.48. Scattering coefficients are computed at scales smaller than a day, and are averaged in time within a day and across days. Figure 8(c) shows $\log_2 \hat{\tilde{S}}X(j_1, j_1 + l)$ as a function of l for different values of j_1 up to largest available scales. The decay of second order coefficients is $\log_2 \hat{\tilde{S}}X(j_1, j_1 + l) \sim -0.2l$ for all $j_2 = j_1 + l$. Contrarily to turbulence data, we do not see an integral scale, beyond which second order coefficients would have a fast decay of $-0.5l$. This is not surprising since the integral scale is known to be larger than few months [5]. Figure 8(d) gives intra-day second order coefficients $j_2 = j_1 + l < 9$. The variance of $\hat{\tilde{S}}X(j_1, j_1 + l)$ is indicated with vertical error bars. Observe that $\log_2 \hat{\tilde{S}}X(j_1, j_1 + l)$ has small variations

²Euro-Bund is one of the most actively traded financial asset in the world. It corresponds to a future contract on an interest rate of the Euro-zone.

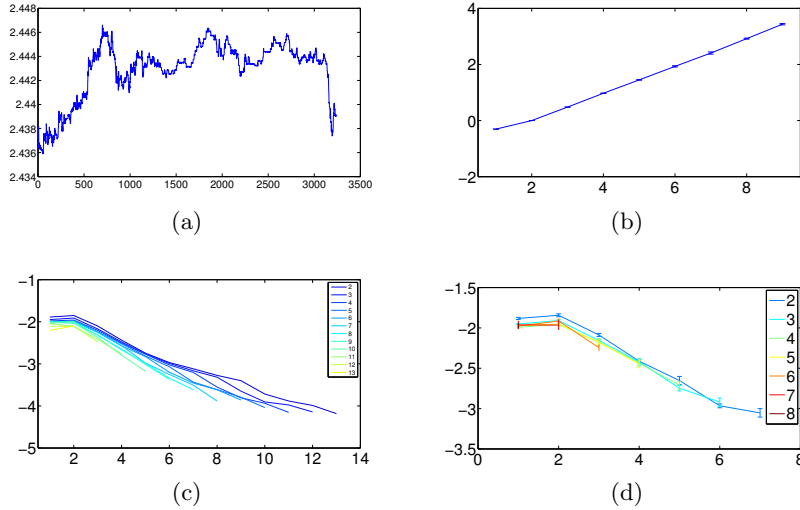


FIG 8. (a) One day of the deseasonalized Euro-Bund log-price $X(t)$. (b) Estimated $\log_2 \tilde{S}X(j_1)$. (c) Estimated $\log_2 \tilde{S}X(j_1, j_1 + l)$. (d) Estimated $\log_2 \tilde{S}X(j_1, j_1 + l)$ for $j_1 + l < 9$.

TABLE 4

The left and right parts of the table correspond to Euro-Bund and S&P 100 time series. The first row gives the estimated parameter value $\hat{\theta}$ for Fractional Brownian Motion (FBM), Levy stable processes (LS) and Multifractal Random Walks (MRW).

S	Euro-Bund			S&P		
	FBM	LS	MRW	FBM	LS	MRW
$\hat{\theta}$	$H = 0.5$	$\alpha = 1.95$	$\lambda^2 = 0.03$	$H = 0.5$	$\alpha = 1.8$	$\lambda^2 = 0.08$
χ_{red}^2	29	26	23	17	16	10

as a function of j_1 , which is a strong indication of self-similarity.

The same scattering computations are performed on the S&P 100 index, sampled every 5 minutes from April 8th 1997 to December 17th 2001 to yield 78 samples every day. Figure 9(a) shows the deseasonalized log price $X(t)$. Panel (b) displays the estimated first order scattering moments. Each trading day has $78 \simeq 2^6$ samples. The deseasonalizing algorithm eliminates opening and closing artifacts and $\log_2 \tilde{S}X(j_1)$ remains regular for j_1 close to 6. Figure 9(c) shows the estimated second order moments. For $j_2 = j_1 + l = 6$ the coefficient $\log_2 \tilde{S}X(j_1, j_1 + l)$ is higher than expected, relatively to other coefficients, which means a higher level of intermittency. As explained in Section 5.1, large scales 2^{j_1} and 2^{j_2} have coefficients of higher variance.

We consider the three following models : (i) fractional Brownian motions

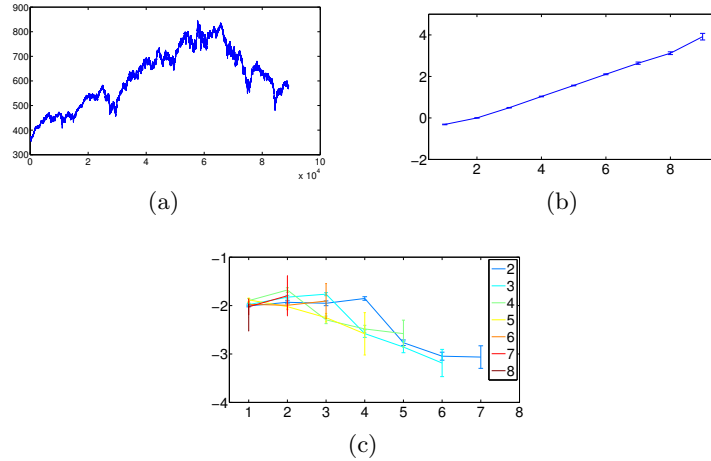


FIG 9. (a) Three years of the deseasonalized S&P 100 index log-price $X(t)$. (b) Estimated $\log_2 \widehat{S}X(j_1)$. (c) Estimated $\log_2 \widehat{S}X(j_1, j_1 + l)$ for $j_1 + l < 9$.

models with $\theta = H$, (ii) Lévy stable processes parametrized with $\theta = \alpha$ and (iii) multifractal random walks with $\theta = \lambda^2$. For each model family, Table 4 estimates an optimal parameter $\hat{\theta}$ from first and second order scattering. They are computed from a total of $N = 3 \cdot 10^6$ (resp. $N = 10^5$) samples for the Euro-Bund (resp. S&P 100). The maximum scale 2^J is adjusted to $J = 8$ (resp. $J = 6$). We set $J_0 = 1$ to eliminate discretization effects in both cases. For fractional Brownian motions, the estimated parameter $\hat{\theta} = H = 0.5$ corresponds to a Brownian motion. Brownian motion models explain the power-spectrum decay of these processes but are known not to be appropriate because they do not take into account the intermittency behavior of financial markets. This appears in the second order scattering coefficients of Figure 8(d) and 9(c), which have a much slower decay than Brownian motions. The Lévy-stable parameters α in Table 4 are close to 2 (order 2 moment of financial time-series are known to be finite). Estimated models of multifractal random walks show the existence of intermittency which is larger for the S&P 100 data set than for the Euro-Bund data.

For each model, Table 4 gives the value of the J-test variable χ_{red}^2 computed with (53). Multifractal random walks have the lowest value χ_{red}^2 for the Euro-Bund and S&P 100 data, which means that these models better fit the data. However, one can not compute a p-value because the empirical covariance matrix is computed from correlated scattering estimators $\widehat{S}X_k$ in (54). Because the integral scale is too large, one cannot fix an interval

Δ providing independent scattering values. One can still verify numerically that the empirical covariance of $\widehat{S}X_k$ converges up to a multiplicative factor, by computing the variations of empirical covariance $\widehat{W}_{\theta,\Delta}^{-1}$ as a function of Δ , and by verifying that

$$\|\widehat{W}_{\theta,\Delta}^{-1} - \eta \widehat{W}_{\theta,\Delta'}^{-1}\| \ll \|\widehat{W}_{\theta,\Delta}^{-1}\|$$

for some $\eta(\Delta, \Delta') \in \mathbb{R}^+$. The ratio between both terms is of the order of 0.05 for the Euro-Bund data.

Appendix A: Proof of Theorem 2.2

Let us first prove (13). If X is a Poisson process then $X \star \psi_j = 2^j dX \star \bar{\psi}_j$ where $\bar{\psi}(t) = \int_0^t \psi(u) du$ has a support in $[-1/2, 1/2]$, and $\bar{\psi}_j(t) = 2^{-j} \bar{\psi}(2^{-j}t)$. Since $dX(t) = \sum_i \delta(t - \tau_i)$ we get $X \star \psi_j(t) = 2^j \sum_i \bar{\psi}_j(t - \tau_i)$. We write

$$(57) \quad |X \star \psi_j(t)| = 2^j |dX \star \bar{\psi}_j|(t) = 2^j (dX \star |\bar{\psi}_j|(t) + e_j(t)) .$$

The first term satisfies

$$(58) \quad \mathbf{E}(dX \star |\bar{\psi}_j|) = \lambda \|\bar{\psi}_j\|_1 = \lambda \|\bar{\psi}\|_1 .$$

Let us show that $\mathbf{E}(|e_j(t)|) = O(\lambda^2 2^j)$. Let $N_j(t)$ be the number of events counted by $X(t)$ in the interval $[t - 2^j, t + 2^j]$. We decompose

$$\mathbf{E}(|e_j(t)|) = \mathbf{E}\left(|e_j(t)| / N_j(t) \leq 1\right) \text{Prob}(N_j(t) \leq 1) + \mathbf{E}\left(|e_j(t)| / N_j(t) > 1\right) \text{Prob}(N_j(t) > 1) .$$

If $N_j(t) \leq 1$, since $\bar{\psi}_j$ has support $[-2^{j-1}, 2^{j-1}]$, it results that $e_j(t) = 0$, and hence $\mathbf{E}\left(|e_j(t)| / N_j(t) \leq 1\right) = 0$. Since

$$|e_j(t)| \leq 2(dX \star |\bar{\psi}_j|(t)) \leq 2^{j+1} \|\bar{\psi}\|_\infty N_j(t) ,$$

it follows that

$$(59) \quad \mathbf{E}(|e_j(t)|) \leq 2\|\bar{\psi}\|_\infty 2^j \mathbf{E}\left(N_j(t) / N_j(t) > 1\right) \text{Prob}(N_j(t) > 1) .$$

Since $N_j(t)$ is a Poisson random variable of parameter $\lambda 2^j$, we verify that

$$\mathbf{E}\left(N_j(t) / N_j(t) > 1\right) \text{Prob}(N_j(t) > 1) = \lambda 2^j (1 - e^{-\lambda 2^j}) ,$$

which implies from (59) that

$$(60) \quad \mathbf{E}(|e_j(t)|) \leq 2\lambda \|\bar{\psi}\|_\infty (1 - e^{-\lambda 2^j}) = O(\lambda^2 2^j) ,$$

and, together with (58) and (57) proves (13).

Property (14) is proved by showing that $2^{-j/2}X \star \psi_j(t)$ converges to a Gaussian random process at large scales 2^j . The convergence of $2^{-j/2}X \star \psi_j(t)$ relies on the use of a central-limit theorem for real dependent random variables. The extension to the two-dimensional complex random variables is done by considering arbitrary linear combinations of its real and imaginary parts. The Cramer-Wold theorem proves that if $X_j = 2^{-j/2}X \star \psi_j(t) = 2^{-j/2}Re(X_j) + i2^{-j/2}Im(X_j)$ satisfies

$$(61) \quad \forall(\alpha, \beta) \in \mathbb{R}^2, \quad \alpha Re(X_j) + \beta Im(X_j) \xrightarrow{j \rightarrow \infty} \alpha A_1 + \beta A_2$$

then $X_j \xrightarrow{j \rightarrow \infty} A_1 + iA_2$. The random variables A_1 and A_2 are zero-mean Gaussian random variables if and only if $\alpha A_1 + \beta A_2$ is a centered Gaussian random variable for all $(\alpha, \beta) \in \mathbb{R}^2$. But

$$\alpha Re(X_j) + \beta Im(X_j) = X \star (\alpha Re(\psi_j) + \beta Im(\psi_j)),$$

so the convergence of X_j to a complex Gaussian variable will follow by showing that $2^{-j/2}X \star \tilde{\psi}_j \rightarrow \mathcal{N}(0, \sigma^2)$ for any wavelet of the form $\tilde{\psi}_j = \alpha Re(\psi_j) + \beta Im(\psi_j)$.

We thus concentrate in the real case, and we denote the real wavelet ψ_j to simplify notations. Assuming $j > 0$,

$$X \star \psi_j(t) = 2^j dX \star \bar{\psi}_j(t) = 2^j \int_{-2^{j-1}}^{2^{j-1}} \bar{\psi}_j(u-t) dX(u) = \sum_{i=-2^{j-1}}^{2^{j-1}-1} S_{i,j},$$

where $S_{i,j} = \int_i^{i+1} \bar{\psi}(2^{-j}(u-t))dX(u)$ are a collection of zero-mean independent random variables. We apply the Berk central limit theorem [?], to this sum of independent random variables.

THEOREM A.1 (Berk Central Limit). *For any $j \in \mathbb{N}$, let $\{S_{i,j}\}_{i=1, \dots, n_j}$ be a sequence of zero mean random variables such that for any $i \leq n_j$ $S_{i,j}$ is independent of $S_{i+r,j}$ for $r \geq m_j$. If the following properties are satisfied*

- (i) $\exists \delta > 0, \lim_{j \rightarrow \infty} n_j^{-1} m_j^{2+2/\delta} = 0$
- (ii) $\exists M > 0, \forall i, j > 0, \mathbf{E}(|S_{i,j}|^{2+\delta}) \leq M$
- (iii) $\exists K > 0, \forall i, j, l > k > 0, \text{Var}(\sum_{i=k+1}^{k+l} S_{i,j}) \leq lK$
- (iv) $\lim_{j \rightarrow \infty} n_j^{-1} \text{Var}(\sum_{i=1}^{n_j} S_{i,j}) = \sigma^2 > 0$

then

$$(62) \quad n_j^{-1/2} \sum_{i=1}^{n_j} S_{i,j} \xrightarrow{j \rightarrow \infty} \mathcal{N}(0, \sigma^2).$$

Let us now verify the hypothesis of this central limit theorem, with $m_j = 1$, $n_j = 2^j$ and $\delta = 1$. Since the variables $(S_{i,j})_i$ are independent, hypothesis (i) is verified with $m_j = 1$. Moreover, we verify that

$$\mathbf{E}(|S_{i,j}|^q) \leq \|\psi\|_\infty^q \mathbf{E}(|N_0|^q)$$

where N_0 is the number of jumps of dX in an interval of length 1. Since it follows a Poisson distribution of parameter λ , it has finite moments. It results that hypothesis (ii) is verified for $\delta = 1$. Since the $S_{i,j}$ are independent, $\text{Var}(\sum_{i=k+1}^{k+l} u_{i,j}) \leq \|\psi\|_\infty^2 l \mathbf{E}(|N_0|^2)$, which verifies hypothesis (iii). Finally, since dX is a white noise of power spectrum λ

$$2^{-j} \sum_{|i| \leq 2^j} \mathbf{E}(|S_{i,j}|^2) = 2^j \mathbf{E}(|dX \star \bar{\psi}_j|^2) = 2^j \sigma^2(dX) \|\bar{\psi}_j\|^2 = \lambda \|\bar{\psi}\|^2 .$$

It verifies the last hypothesis (iv). Applying (A.1) and the Cramer-Wald theorem proves that $2^{-j/2} X \star \psi_j(t)$ converges to a complex Gaussian distribution of total variance $\lambda \|\bar{\psi}\|^2$. In order to control the limit of first order moments, we use the following lemma on uniform integrability of sequences of random variables:

LEMMA A.2. ([11], thm 6.1-6.2) *Let $\{X_j\}_{j \in \mathbb{N}}$ be a sequence of random variables. If $X_j \xrightarrow{d} X_\infty$ and*

$$\sup_j \mathbf{E}(|X_j|^{1+\delta}) < \infty \text{ for } \delta > 0 ,$$

then

$$\lim_{j \rightarrow \infty} \mathbf{E}(X_j) = \mathbf{E}(X_\infty) .$$

As a result, for any $\alpha \leq 2$, $\mathbf{E}(|2^{-j/2} X \star \psi_j|^\alpha) \rightarrow \mathbf{E}(|Z_1 + iZ_2|^\alpha)$, where Z_1 and Z_2 are Gaussian random variables with total variance $\lambda \|\bar{\psi}\|^2$. For $\alpha = 1$, it results that there exists a constant C , depending only on the wavelet ψ , such that

$$\lim_{j \rightarrow \infty} 2^{-j/2} \mathbf{E}(|X \star \psi_j|) = \lambda^{1/2} \|\bar{\psi}\| C .$$

which proves (14).

The proof of (15) is very similar to the proof of (13). The key property is that $||X \star \psi_{j_1}| \star \psi_{j_2}|$ only depends on values of X over an interval of size $2^{j_1} + 2^{j_2}$. From (60), it results that

(63)

$$|X \star \psi_{j_1}| \star \psi_{j_2}(t) = 2^{j_1} |dX \star \bar{\psi}_{j_1}| \star \psi_{j_2}(t) \stackrel{d}{=} 2^{j_1} (dX \star (|\bar{\psi}_{j_1}| \star \psi_{j_2})(t) + e_{j_1} \star \psi_{j_2}) ,$$

with $\mathbf{E}(|e_{j_1} \star \psi_{j_2}|) = O(\lambda^2 2^{j_1})$. As a consequence, (63) and (13) imply that

$$(64) \quad \begin{aligned} \mathbf{E}(|X \star \psi_{j_1} \star \psi_{j_2}(t)|) &= 2^{j_1} (\mathbf{E}(|dX \star (|\bar{\psi}_{j_1}| \star \psi_{j_2})|(t)) + O(\lambda^2 2^{j_1})) , \\ &= 2^{j_1} \lambda \|(|\bar{\psi}_{j_1}| \star \psi_{j_2})\|_1 (1 + O(\lambda 2^{j_1}) + O(\lambda 2^{j_2})) . \end{aligned}$$

Using again (13), we conclude that

$$\begin{aligned} \tilde{S}X(j_1, j_2) &= \frac{\mathbf{E}(|dX \star \bar{\psi}_{j_1}| \star \psi_{j_2}(t)|)}{\mathbf{E}(|dX \star \bar{\psi}_{j_1}|)} \\ &= \frac{\|(|\bar{\psi}| \star \psi_{j_2-j_1})\|_1}{\|\bar{\psi}\|_1} (1 + O(\lambda 2^{j_1}) + O(\lambda 2^{j_2})) , \end{aligned}$$

which proves (15). Finally, in order to prove (16), observe that $|X \star \psi_j|$ is a stationary process with lag 2^j . As a result, by using the same Central Limit argument to prove (14), one can verify that $2^{j_2/2}(|X \star \psi_{j_1}| \star \psi_{j_2})$ converges in distribution towards a Gaussian distribution as $j_2 \rightarrow \infty$, which yields a decay on the normalized second order scattering of the form $\tilde{S}dX(j_1, j_2) \simeq 2^{-j_2/2}$ as $j_2 \rightarrow \infty$. \square

Appendix B: Proof of lemma 3.3

Let $Y_j(t) = 2^{j/2} |dB \star \varphi| \star \psi_j(t)$. To prove that $\mathbf{E}(|Y_j|)$ converges to a constant, we shall prove that the distribution of Y_j is asymptotically Gaussian:

$$(65) \quad Y_j(t) \xrightarrow{j \rightarrow \infty} A = A_1 + iA_2$$

where A_1 and A_2 are two zero-mean Gaussian distributions of total variance $\sigma_1^2 + \sigma_2^2 = \|\psi\|_2^2 \int R_{|dB \star \varphi|}(\tau) d\tau$, which is the first result of Lemma 3.3. We shall also prove that

$$(66) \quad \lim_{j \rightarrow \infty} \mathbf{E}(|Y_j|^2) = \mathbf{E}(|A|^2).$$

Using again lemma (A.2), we conclude that

$$(67) \quad \lim_{j \rightarrow \infty} \mathbf{E}(|Y_j|) = \mathbf{E}(|A|) > 0 .$$

and hence finish the proof of Lemma 3.3.

For that purpose, we follow the same strategy as in the proof of (14), applied to the process $Y_j = 2^{j/2} |dB \star \varphi| \star \bar{\psi}_j(t)$, where $\bar{\psi}_j$ is any linear combination of real and imaginary parts of ψ_j .

Let us write $\varphi_\Delta = \varphi \mathbf{1}_{[-\Delta/2, \Delta/2]}$. We shall limit ϕ to a compact support by defining $\{\Delta_j\}_{j \geq 0}$ with $\lim_{j \rightarrow \infty} \Delta_j = \infty$ and decompose

$$|dB \star \varphi(t)| = |dB \star \varphi_{\Delta_j} + dB \star (\varphi - \varphi_{\Delta_j})| .$$

As a result

$$|dB \star \varphi(t)| = |dB \star \varphi_{\Delta_j}| + Z_j(t)$$

with $\mathbf{E}(|Z_j|) \leq \mathbf{E}(|dB \star (\varphi - \varphi_{\Delta_j})|)$. Since dB is the Wiener measure, if $\theta \in \mathbf{L}^2(\mathbb{R})$ then

$$(68) \quad \mathbf{E}(|dB \star \theta|) \leq \mathbf{E}(|dB \star \theta|^2)^{1/2} = \|\theta\|_2 ,$$

so $\mathbf{E}(|Z_j|) \leq \|\varphi - \varphi_{\Delta_j}\|_2$. It results that

$$(69) \quad |dB \star \varphi| \star \bar{\psi}_j(t) = |dB \star \varphi_{\Delta_j}| \star \bar{\psi}_j(t) + Z_j \star \bar{\psi}_j(t) ,$$

and

$$\mathbf{E}(|Z_j \star \bar{\psi}_j|) \leq \mathbf{E}(|Z_j|) \|\bar{\psi}_j\|_1 \leq \|\varphi - \varphi_{\Delta_j}\|_2 \|\bar{\psi}\|_1 .$$

Since $\lim_{j \rightarrow \infty} \Delta_j = \infty$, $\lim_{j \rightarrow \infty} \|\varphi - \varphi_{\Delta_j}\|_2 = 0$ so $Z_j \star \bar{\psi}_j$ converges to 0 in probability when j increases. So the limits of $|dB \star \varphi| \star \bar{\psi}_j(t)$ and $|dB \star \varphi_{\Delta_j}| \star \bar{\psi}_j(t)$ are equal.

We now prove (24) by applying Berk central limit Theorem A.1, to show that $\bar{Y}_j = |dB \star \varphi_{\Delta_j}| \star \bar{\psi}_j(t)$ converges to a normal distribution. Since $|dB \star \varphi_{\Delta_j}| \star \bar{\psi}_j(t)$ is stationary, its distribution can be evaluated at $t = 0$

$$|dB \star \varphi_{\Delta_j}| \star \bar{\psi}_j(0) = \int |dB \star \varphi_{\Delta_j}|(u) \bar{\psi}_j(-u) du .$$

The central-limit theorem is applied by dividing this integral into disjoint integrals

$$(70) \quad S_{i,j} = 2^j \int_{2^j b_{i,j}}^{2^j b_{i+1,j}} |dB \star \varphi_{\Delta_j}|(u) \bar{\psi}_j(-u) du ,$$

where for each $j \in \mathbb{Z}$, $\{b_{i,j}\}_{1 \leq i \leq n_j}$ is an increasing sequence of points in $\mathbb{R} \cup \{\pm\infty\}$ such that

$$(71) \quad \forall i , \int_{b_{i,j}}^{b_{i+1,j}} |\bar{\psi}(-u)| du = 2^{-j} \|\bar{\psi}\|_1 .$$

Since $\bar{\psi}$ is \mathbf{C}^1 and bounded, we verify that $n_j \simeq 2^j$. Summing these random variables gives

$$(72) \quad 2^{-j/2} \sum_{i=1}^{n_j} S_{i,j} = 2^{j/2} |dB \star \varphi_{\Delta_j}| \star \bar{\psi}_j(0) .$$

We now show that the $S_{i,j}$ satisfy the hypothesis of the Beck central-limit theorem so that we can apply the convergence result (62) which implies (24).

Let us first prove that $S_{i,j}$ is independent of $S_{i+r,j}$ for $r \geq m_j$ which satisfies (i). Since $\bar{\psi}$ is bounded, it results that $\inf_{i,j} 2^j |b_{i,j} - b_{i+1,j}| = \eta > 0$. Since φ_{Δ_j} has a support of size Δ_j and dB is a Wiener Noise, it follows that $|dB \star \varphi_{\Delta_j}|(u)$ is independent of $|dB \star \varphi_{\Delta_j}|(u')$ for $|u - u'| > \Delta_j$ and hence that $S_{i,j}$ is independent of $S_{i+r,j}$ for $r \geq m_j = \Delta_j/\eta$.

To verify (i) let us set $\delta = 1$. Since $n_j \simeq 2^j$, if we choose $\Delta_j = 2^{j/5}$ then

$$(73) \quad \lim_{j \rightarrow \infty} \frac{m_j^4}{n_j} \leq \eta^{-4} \lim_{j \rightarrow \infty} 2^{j(4/5-1)} = 0 .$$

We now verify condition (ii) with $\delta = 1$. Since $\bar{\psi}_j(u)$ has a zero integral, one can replace $|dX \star \varphi_{\Delta_j}(u)|$ by $Q_j(u) = |dX \star \varphi_{\Delta_j}|(u) - \mathbf{E}(|dX \star \varphi_{\Delta_j}|)$ in the definition (70) of $S_{i,j}$. It results that

$$\begin{aligned} \mathbf{E}(|S_{i,j}|^3) &\leq \iiint \mathbf{E}(Q_j(u)Q_j(u')Q_j(u'')) 2^{3j} |\bar{\psi}_j(-u)| |\bar{\psi}_j(-u')| |\bar{\psi}_j(-u'')| du du' du'' \\ &\leq \mathbf{E}(|dB \star \varphi_{\Delta_j}|^3) \|\bar{\psi}\|_1^3 = 2^{5/2} \pi^{-1/2} \|\varphi_{\Delta_j}\|_2^3 \|\bar{\psi}\|_1^3 \leq 2^{5/2} \pi^{-1/2} \|\varphi\|_2^3 \|\bar{\psi}\|_1^3 . \end{aligned}$$

Let us now verify condition (iii). The sum $A_{k,l,j} = \sum_{i=k}^{k+l} S_{i,j}$ is by definition

$$A_{k,l,j} = 2^j \int_{2^j b_{k,j}}^{2^j b_{k+l,j}} |dB \star \varphi_{\Delta_j}(u)| \bar{\psi}_j(-u) du = \int_{\mathbb{R}} |dB \star \varphi_{\Delta_j}(u)| h_{k,l,j}(u) du$$

with $h_{k,l,j}(u) = 2^j \bar{\psi}_j(-u) 1_{[2^j b_{k,j}, 2^j b_{k+l,j}]}(u)$. It results that

$$(74) \quad \text{Var}(A_{k,l,j}) \leq \|R_{|dB \star \varphi_{\Delta_j}|}\|_1 \|h_{k,l,j}\|_2^2 .$$

But, with a change of variable and applying (71) we get

$$\|h_{k,l,j}\|_2^2 = \int_{2^j b_{k,j}}^{2^j b_{k+l,j}} |\bar{\psi}(2^{-j}u)|^2 du \leq \|\bar{\psi}\|_\infty \int_{b_{k,j}}^{b_{k+l,j}} 2^j |\bar{\psi}(u)| du \leq \|\bar{\psi}\|_\infty \|\bar{\psi}\|_1 l .$$

We are now going to bound $\|R_{|dB \star \varphi_{\Delta_j}|}\|_1$ by using the decay $\varphi(u) = O((1 + |u|^{-2}))$.

$$R_{|dB \star \varphi_{\Delta_j}|}(\Delta) = \mathbf{E}(|dB \star \varphi_{\Delta_j}(\Delta)| |dB \star \varphi_{\Delta_j}(0)|) - \mathbf{E}(|dB \star \varphi_{\Delta_j}|)^2 .$$

If $|\Delta| > |\Delta_j|$ then since the support of $\varphi_{\Delta_j}(u)$ and $\varphi_{\Delta_j}(u - \Delta)$ does not overlap, $|dB \star \varphi_{\Delta_j}(\Delta)|$ and $|dB \star \varphi_{\Delta_j}(0)|$ are independent random variables so $R_{|dB \star \varphi_{\Delta_j}|}(\Delta) = 0$. Otherwise, we decompose

$$|dB \star \varphi_{\Delta_j}(u)| = |dB \star \varphi_{\Delta}(u) + dB \star (\varphi_{\Delta_j} - \varphi_{\Delta})(u)| .$$

Since $|dB \star \varphi_\Delta(0)|$ and $|dB \star \varphi_\Delta(\Delta)|$ are independent random variables,

$$\begin{aligned} |R_{|dB \star \varphi_{\Delta_j}|}(\Delta)| &\leq |\mathbf{E}(|dB \star \varphi_\Delta|)^2 - \mathbf{E}(|dB \star \varphi_{\Delta_j}|)^2| + \\ &\quad + 2\mathbf{E}(|dB \star \varphi_\Delta|)\mathbf{E}(|dB \star (\varphi_{\Delta_j} - \varphi_\Delta)|) + \mathbf{E}(|dB \star (\varphi_{\Delta_j} - \varphi_\Delta)|)^2 . \end{aligned}$$

Since $\mathbf{E}(|dB \star \theta|) \leq \mathbf{E}(|dB \star \theta|^2)^{1/2} \leq \|\theta\|_2$, by applying this to $\theta = \varphi_\Delta$ and $\theta = \varphi_{\Delta_j} - \varphi_\Delta$ one can verify that

$$(75) \quad |R_{|dB \star \varphi_{\Delta_j}|}(\Delta)| \leq 6\|\varphi\|_2 \|\varphi - \varphi_\Delta\|_2 .$$

Since $\varphi(u) = O((1 + |u|)^{-2})$ it results that $\|\varphi - \varphi_\Delta\|_2 = O((1 + |\Delta|)^{-3/2})$ so $\|R_{|dB \star \varphi_{\Delta_j}|}\|_1$ is bounded independently of j . Inserting this in (74) proves the theorem hypothesis (iii).

Let us now verify the hypothesis (iv). It results from (72) that

$$2^{-j} \text{Var}\left(\sum_i S_{i,j}\right) = 2^j \text{Var}(|dX \star \varphi_{\Delta_j}| \star \bar{\psi}_j) = 2^j \int \widehat{R}_{|dX \star \varphi_{\Delta_j}|}(\omega) |\widehat{\bar{\psi}}(2^j \omega)|^2 d\omega .$$

We proved (75) that $R_{|dB \star \varphi_{\Delta_j}|} \in \mathbf{L}^1$ but the same inequality is valid for $R_{|dB \star \varphi_\Delta|}$ which proves that it is also in \mathbf{L}^1 . It results that $\widehat{R}_{|dX \star \varphi|}$ is continuous. Since φ_{Δ_j} converges to φ in $\mathbf{L}^2 \cap \mathbf{L}^1$ as $j \rightarrow \infty$, $\widehat{R}_{|dX \star \varphi_j|}(0)$ converges to $\widehat{R}_{|dX \star \varphi|}(0)$. Since $2^j |\widehat{\bar{\psi}}(2^j \omega)|^2$ converges to $\|\bar{\psi}\|_2^2 \delta(\omega)$ when j goes to ∞

$$\lim_{j \rightarrow \infty} 2^{-j} \text{Var}\left(\sum_i S_{i,j}\right) = \widehat{R}_{|dX \star \varphi|}(0) \|\bar{\psi}\|_2^2 = \bar{\sigma}^2 ,$$

which proves condition (iv).

We can thus apply Theorem A.1 which proves that $2^{j/2} |dB \star \varphi| \star \bar{\psi}_j(t)$ converges in distribution to $\mathcal{N}(0, \bar{\sigma}^2)$ and hence (24). Finally, by following the same reasoning used in Theorem 2.2, we apply Lemma A.2 to conclude that $\lim_{j \rightarrow \infty} 2^{j/2} \mathbf{E}(|dB \star \varphi| \star \psi_j) = C > 0$, which proves (25) \square .

Appendix C: Various results on the MRM measure

LEMMA C.1. *The process $\omega_t^T(t)$ used for the construction of the MRM dM is an infinitely-divisible process whose two-points characteristic function reads:*

$$(76) \quad \mathbf{E}\left(e^{p_1 \omega_t^T(t_1) + p_2 \omega_t^T(t_2)}\right) = e^{[F(p_1) + F(p_2)] \rho_t^T(0) + [F(p_1 + p_2) - F(p_1) - F(p_2)] \rho_t^T(t_2 - t_1)}$$

where $F(-ip)$ is the cumulant generating function characterizing the infinitely divisible law as provided by the Levy-Khintchine formula where the drift term is chosen such that

$$(77) \quad F(1) = 0 ,$$

and where the function $\rho_l^T(\tau)$ is defined by:

$$(78) \quad \rho_l^T(\tau) = \begin{cases} \ln(T/l) + 1 - |\tau|/l , & \text{if } |\tau| \leq l , \\ \ln(T/|\tau|) , & \text{if } l \leq |\tau| < T , \\ 0 , & \text{otherwise .} \end{cases}$$

Moreover, the function $\zeta(p)$ which satisfies (32) (with $X = dM$ where dM is the associated MRM) is given by

$$\zeta(p) = p - F(p).$$

The proof of this Lemma is given in [6].

The next Lemma uses an alternative MRM measure considered in Ref. [6] defined by

$$d\tilde{M}(t) = \lim_{l \rightarrow 0} e^{\tilde{\omega}_l^T(t)} dt$$

where $\tilde{\omega}_l^T$ is defined exactly as the process ω_l^T but only differs by its ρ function which is replaced by : $\tilde{\rho}_l^T(\tau) = \rho_l^T(\tau) + \frac{\tau}{T} - 1$, for $\tau \leq T$. One can then easily show that $\tilde{\omega}_l^T$ is linked with ω_l^T by the following cascade property :

$$(79) \quad \forall l \leq a \leq T, \omega_l^T(u) \stackrel{a.s.}{=} \tilde{\omega}_l^a(u) + \omega_a^T(u)$$

where $\tilde{\omega}_l^a$ and ω_a^T are independent copies of the processes defined previously. Moreover, $\tilde{\omega}_l^T$ satisfies both (37) and (37).

We are now ready to state the last Lemma we will need.

LEMMA C.2. *Let ω_l^T the infinitely divisible process associated with the MRM dM and ψ be a wavelet of support in $[0, 1]$ such that $\|\psi\|_\infty < \infty$. For all α such that $0 < \alpha < 1$, one has:*

$$(80) \quad \forall l < 2^j, (\psi_j \star e^{\omega_l^T})(t) = e^{\omega_{2^j}^T(t)} \left(\psi_j \star e^{\tilde{\omega}_l^{2^j \alpha}} \right) + \eta_{l,j}(t) ,$$

where the process $\eta_{l,j}(t)$ has a limit process $\lim_{l \rightarrow 0} \eta_{l,j}(t) = \eta_j(t)$ which satisfies, in the limit $j \rightarrow -\infty$,

$$(81) \quad \mathbf{E}(|\eta_j(t)|) = O(2^{j \frac{1-\alpha(1+F(2))}{2}})$$

and

$$(82) \quad \mathbf{E}(|\eta_j(t)|^2) = O(2^{j(3-F(2)-\alpha)}) .$$

Without loss of generality we fix $t = 0$. Let us consider $0 < \alpha < 1$ and l and j small enough and such that:

$$l < 2^j < 2^{j\alpha} < T$$

Let us first remark that, for $u < 2^{j\alpha}$, one has from (76):

$$(83) \quad \mathbf{E} \left(e^{p(\omega_{2^{j\alpha}}^T(u) + \omega_{2^{j\alpha}}^T(0))} \right) = 2^{-j\alpha F(2p)} T^{F(2p)} e^{F(2p)(1-u2^{-j\alpha})}$$

where $F(p) = \varphi(-ip) = p - \zeta(p)$. Hence, we have:

$$\begin{aligned} \mathbf{E} \left(e^{2\omega_{2^{j\alpha}}^T(u)} \right) &= 2^{-j\alpha F(2)} T^{F(2)} e^{F(2)} \\ \mathbf{E} \left(e^{\omega_{2^{j\alpha}}^T(u) + \omega_{2^{j\alpha}}^T(0)} \right) &= 2^{-j\alpha F(2)} T^{F(2)} e^{F(2)(1-u2^{-j\alpha})} . \end{aligned}$$

One defines $\eta_{l,j}$ as:

$$(84) \quad \eta_{l,j}(0) = 2^{-j} \int \psi(u2^{-j}) \left(e^{\omega_l^T(u)} - e^{\tilde{\omega}_l^{2^{j\alpha}}(u) + \omega_{2^{j\alpha}}^T(0)} \right) du$$

Using dominated convergence, (79), $\mathbf{E}(e^{\tilde{\omega}_l^{2^{j\alpha}}}) = 1$ and the fact that ψ is a bounded function of support $[0, 1]$ one has:

$$\begin{aligned} \mathbf{E}(\lim_{l \rightarrow 0} |\eta_{l,j}|) &= \lim_{l \rightarrow 0} \mathbf{E}(|\eta_{l,j}|) \\ &\leq \|\psi\|_\infty 2^{-j} \int_0^{2^j} \sqrt{\mathbf{E} \left[\left(e^{\omega_{2^{j\alpha}}^T(u)} - e^{\omega_{2^{j\alpha}}^T(0)} \right)^2 \right]} du \\ &= \|\psi\|_\infty 2^{-j} \int_0^{2^j} \sqrt{\mathbf{E} \left(e^{2\omega_{2^{j\alpha}}^T(0)} + e^{2\omega_{2^{j\alpha}}^T(u)} - 2e^{\omega_{2^{j\alpha}}^T(u) + \omega_{2^{j\alpha}}^T(0)} \right)} du \\ &= \sqrt{2} \|\psi\|_\infty 2^{-\frac{j\alpha F(2)}{2}} T^{\frac{F(2)}{2}} e^{\frac{F(2)}{2}} \int_0^1 \left(1 - e^{-F(2)u2^{j(1-\alpha)}} \right)^{\frac{1}{2}} du \\ &\underset{j \rightarrow -\infty}{=} O(2^{j \frac{1-\alpha(1+F(2))}{2}}) \end{aligned}$$

which proves (81). In order to bound the second moment, we consider

$$\begin{aligned}
& \mathbf{E}(\lim_{l \rightarrow 0} |\eta_{l,j}|^2) = \lim_{l \rightarrow 0} \mathbf{E}(|\eta_{l,j}|^2) \\
= & 2^{-2j} \iint_0^{2^j} \psi(2^{-j}u) \psi(2^{-j}u') \mathbf{E}(e^{\tilde{\omega}_l^{2j\alpha}(u) + \tilde{\omega}_l^{2j\alpha}(u')}) \mathbf{E}\left((e^{\omega_{2j\alpha}^T(u)} - e^{\omega_{2j\alpha}^T(0)})(e^{\omega_{2j\alpha}^T(u')} - e^{\omega_{2j\alpha}^T(0)})\right) dud u' \\
\leq & 2^{-2j} 2^{-j\alpha F(2)} (Te)^{F(2)} \iint_0^{2^j} |\psi(2^{-j}u)| |\psi(2^{-j}u')| \mathbf{E}(e^{\tilde{\omega}_l^{2j\alpha}(u) + \tilde{\omega}_l^{2j\alpha}(u')}) \cdot \\
& \cdot \left| e^{-F(2)|u-u'|2^{-j\alpha}} + 1 - e^{-F(2)|u|2^{-j\alpha}} - e^{-F(2)|u'|2^{-j\alpha}} \right| dud u' \\
= & 2^{-j\alpha F(2)} (Te)^{F(2)} \iint_0^1 |\psi(u)| |\psi(u')| \mathbf{E}(e^{\tilde{\omega}_l^{2j\alpha}(2^j u) + \tilde{\omega}_l^{2j\alpha}(2^j u')}) \cdot \\
& \cdot \left| e^{-F(2)|u-u'|2^{j(1-\alpha)}} + 1 - e^{-F(2)|u|2^{j(1-\alpha)}} - e^{-F(2)|u'|2^{j(1-\alpha)}} \right| dud u' \\
= &_{j \rightarrow -\infty} O(2^{j(1-\alpha(1+F(2)))}) \mathbf{E}(|e^{\tilde{\omega}_l^{2j\alpha}(2^j u)} \star |\psi|^2|) \\
= & O(2^{j(1-\alpha(1+F(2))+\zeta(2)+\alpha F(2))}) = O(2^{j(3-F(2)-\alpha)}) . \quad \square
\end{aligned}$$

Let us remark that one could obtain a smaller error with a smoother variant of the ω_l . Indeed, as shown in [35] it is possible to choose the way ω_l is regularized at scale l . One can thus define a MRM process using ω_l with a covariance function that is C^2 at $\tau = 0$. In that case, in (83), the function $\rho_l(u)$ would be proportional to $2^{-2j\alpha}u^2$ and the error mean absolute value could be bounded by $2^{j(1-\alpha-F(2)/2)}$.

Appendix D: Proof of Theorem 4.2

D.1. Proof of (i). We first prove that for all $t \in [0, 2^L - 1]$ and all $j < L$

$$(85) \quad \frac{dM \star \psi_j}{\mathbf{E}(|dM \star \psi|)} \stackrel{law}{=} e^{\Omega_{2^j-L}} \xi(t 2^{-j}) ,$$

where Ω_s is the random variable defined in (38) and $\xi_1(t)$ is a normalized 1-dependent, stationary random process independent of Ω_{2^j-L} defined as:

$$(86) \quad \xi(t) = K^{-1} \epsilon_1(t)$$

where $\epsilon_1(t) = \lim_{l \rightarrow 0} \int \psi(u-t) e^{\omega_l^1(u)} du$ and $K = \mathbf{E}(|\epsilon_1(t)|)$.

Let $j < L$ and $dM_l = e^{\omega_l^{2^j}(t)} dt$. From (37), one has:

$$dM_l \star \psi_j \stackrel{law}{=} 2^{-j} \int e^{\omega_{2^j-L}^{2^j}(u 2^{j-L})} \psi(2^{-j}(t-u)) du ,$$

and thus, by setting $s = 2^{j-L}$, from (38) and (37):

$$dM_l \star \psi_j \stackrel{\text{law}}{=} 2^{-j} e^{\Omega_s} \int \psi(2^{-j}(t-u)) e^{\omega_l^{2^j}(u)} du \stackrel{\text{law}}{=} e^{\Omega_s} \int \psi(2^{-j}t-u) e^{\omega_{l2^{-j}}^1(u)} du .$$

Taking the limit $l \rightarrow 0$ for a fixed j in the last equation shows that

$$(87) \quad dM \star \psi_j \stackrel{\text{law}}{=} e^{\Omega_{2^{j-L}}} \epsilon_1(t2^{-j}) ,$$

with

$$(88) \quad \epsilon_T(t) = \lim_{l \rightarrow 0} \int \psi(u-t) e^{\omega_l^T(u)} du .$$

Normalizing $\epsilon_1(t)$ by $E(|dM \star \psi|)$ proves (85).

Since ψ has a compact support of size 1, the process $\epsilon_1(t)$ (and therefore the process $\xi_1(t)$) is a 1-dependent process, i.e., $\forall \tau > 1$, $\epsilon_1(t+\tau)$ is independent from $\{\epsilon_1(t')\}_{t' \leq t}$. Equation (39) is a direct consequence of (85) and of the fact that $E(e^{\Omega_s}) = 1$. \square

D.2. Proof of (ii). As for the first order, using first (37) and then (38) with $s = 2^{j_2-L}$ we obtain :

$$\begin{aligned} |\psi_{j_2} \star |\psi_{j_1} \star dM_l|| (t) &\stackrel{\text{law}}{=} |\psi_{j_2} \star |\psi_{j_1} \star dM_l|| (0) \\ &\stackrel{\text{law}}{=} 2^{-j_2} e^{\Omega_{2^{j_2-L}}} \left| \int \psi(-u2^{-j_2}) 2^{-j_1} \left| \int \psi\left(\frac{u-v}{2^{j_1}}\right) e^{\omega_l^{2^{j_2}}(v)} dv \right| du \right| . \end{aligned}$$

Making the changes of variables $u' = u2^{-j_2}$ and $v' = v2^{-j_1}$ and using (37), leads to

$$|\psi_{j_2} \star |\psi_{j_1} \star dM_l|| (t) \stackrel{\text{law}}{=} e^{\Omega_{2^{j_2-L}}} \left| \int \psi(-u) \left| \int \psi(2^{j_2-j_1}u-v) e^{\omega_{2^{-j_1}l}^{2^{j_2}}(v)} dv \right| du \right| .$$

Since j_2 is fixed, with no loss of generality, in the following we can set $j_2 = 0$. Using (37), one gets

$$(89) \quad |\psi \star |\psi_{j_1} \star dM_l(0)|| \stackrel{\text{law}}{=} e^{\Omega_{2^{-L}}} \left| \int \psi(-u) |\psi_{j_1} \star e^{\omega_l^1(u)}| du \right| .$$

We now use the Lemma C.2 proved in Appendix C with $\alpha = \frac{1-2\nu}{1+F(2)}$ ($\nu < 1/2$). We get :

$$(90) \quad \mathbf{E}(|\eta_{j_1}|) = O(2^{j_1\nu}) ,$$

and

$$\begin{aligned}
\psi_{j_1} \star e^{\omega_t^1}(u) &= 2^{-j_1} e^{\omega_{2^{j_1}}^1(u)} \int \psi\left(\frac{u-v}{2^{j_1}}\right) e^{\tilde{\omega}_t^{2^{j_1}\alpha}(v)} dv + \eta_{j_1,l}(u) \\
&\stackrel{law}{=} e^{\omega_{2^{j_1}}^1(u)} \int \psi(u2^{-j_1} - v) e^{\tilde{\omega}_{t2^{-j_1}}^1(v2^{j_1(1-\alpha)})} dv + \eta_{j_1,l}(u) \\
&\stackrel{law}{=} e^{\omega_{2^{j_1}}^1(u)} \int \psi(u2^{-j_1} - v) e^{\tilde{\omega}_{t2^{-j_1}}^{2^{j_1}(\alpha-1)}(v)} dv + \eta_{j_1,l}(u) \\
&\xrightarrow{l \rightarrow 0} e^{\omega_{2^{j_1}}^1(u)} \tilde{\epsilon}_{2^{j_1}(\alpha-1)}(2^{-j_1}u) + \eta_{j_1}(u) ,
\end{aligned}$$

where we used property (37) for $\tilde{\omega}_t^T$ and we defined the T -dependent noise:

$$(91) \quad \tilde{\epsilon}_T(t) = \lim_{l \rightarrow 0} \int \psi(t-v) e^{\tilde{\omega}_{t2^{-j_1}}^T(v)} dv .$$

It follows that :

$$\lim_{l \rightarrow 0} \psi \star |\psi_{j_1} \star dM_l(0)| \stackrel{law}{=} e^{\Omega_{2^{-L}}} \int \psi(-u) e^{\omega_{2^{j_1}}^1(u)} |\tilde{\epsilon}_{2^{j_1}(\alpha-1)}(2^{-j_1}u)| du + \int \psi(-u) \tilde{\eta}_{j_1}(u) du ,$$

where

$$(92) \quad \tilde{\eta}_{j_1}(u) = |e^{\omega_{2^{j_1}}^1(u)} \tilde{\epsilon}_{2^{j_1}(\alpha-1)}(2^{-j_1}u) + \eta_{j_1}(u)| - |\tilde{\epsilon}_{2^{j_1}(\alpha-1)}(2^{-j_1}u)| .$$

Along the same line as in ref [31, 6], it is easy to prove that in the limit $T \rightarrow \infty$:

$$(93) \quad \mathbf{E}(|\tilde{\epsilon}_T(t)|^q) \simeq \tilde{K}_q T^{q-\zeta(q)} ,$$

where \tilde{K}_q does not depend on T (thanks to the stationarity of $\tilde{\epsilon}_T(t)$, it does not depend on t either). Since $\zeta(1) = 1$, let $\tilde{K}_1 = \tilde{K} = \mathbf{E}(|\tilde{\epsilon}_T(t)|)$ and let us define the centered process: $\bar{\epsilon}_T(t) = |\tilde{\epsilon}_T(t)| - \tilde{K}$. Let us remark that, when $T \rightarrow \infty$,

$$(94) \quad \mathbf{E}(\bar{\epsilon}_T^2) \simeq \mathbf{E}(\tilde{\epsilon}_T^2) \simeq T^{2-\zeta(2)} .$$

Thus we can write

$$(95) \quad \lim_{l \rightarrow 0} \psi \star |\psi_{j_1} \star dM_l(0)| \stackrel{law}{=} e^{\Omega_{2^{-L}}} (I + II + III) ,$$

where

$$(96) \quad I = \tilde{K} \int \psi(-u) e^{\omega_{2^{j_1}}^1(u)} du ,$$

$$(97) \quad II = \int \psi(-u) e^{\omega_{2^{j_1}}^1(u)} \bar{\epsilon}_{2^{j_1}(\alpha-1)}(2^{-j_1}u) du ,$$

$$(98) \quad III = \int \psi(-u) \tilde{\eta}_{j_1}(u) du .$$

Since $\int \psi(u) e^{\omega_{2^{j_1} \alpha}^1} du$ converges in law, when $j_1 \rightarrow -\infty$, towards $\epsilon_1(t)$, (where $\epsilon_1(t)$ is an independent copy of the process defined in (88)), we have, in the limit $j_1 \rightarrow -\infty$:

$$(99) \quad \mathbf{E}(|I|) \rightarrow K \tilde{K} ,$$

where $K = \mathbf{E}(|\epsilon_1(t)|)$. Thus, since $\bar{S}dM(j_1, 0) = \mathbf{E}(|I + II + III|)$,

$$|\bar{S}dM(j_1, 0) - \tilde{K}K| \leq |\mathbf{E}(|I + II|) - \mathbf{E}(|I|)| + \mathbf{E}(|III|) .$$

From the Lemma, we know that $\lim_{j_1 \rightarrow -\infty} \mathbf{E}(|\eta_{j_1}|) = 0$ and consequently $\lim_{j_1 \rightarrow -\infty} \mathbf{E}(|\tilde{\eta}_{j_1}|) = 0$ which leads to $\lim_{j_1 \rightarrow -\infty} \mathbf{E}(|III|) = 0$. Moreover

$$|\mathbf{E}(|I + II|) - \mathbf{E}(|I|)| \leq \mathbf{E}(|II|) \leq \sqrt{\mathbf{E}(|II|^2)} .$$

From the expression of II and the fact that $\bar{\epsilon}_{2^{j_1(\alpha-1)}}(2^{-j_1}u)$ is a $2^{j_1\alpha}$ -dependent process, we have, when $j_1 \rightarrow -\infty$:

$$\begin{aligned} \mathbf{E}(|II|^2) &\leq \|\psi\|_\infty^2 \int_0^1 \int_0^1 \mathbf{E} \left(e^{\omega_{2^{j_1} \alpha}^1(u) + \omega_{2^{j_1} \alpha}^1(v)} \right) \mathbf{E} \left(\bar{\epsilon}_{2^{j_1(\alpha-1)}}(2^{-j_1}u) \bar{\epsilon}_{2^{j_1(\alpha-1)}}(2^{-j_1}v) \right) dudv \\ &\leq \|\psi\|_\infty^2 \mathbf{E}(\bar{\epsilon}_{2^{j_1(\alpha-1)}}^2) 2^{j_1\alpha} \mathbf{E}(e^{2\omega_{2^{j_1} \alpha}^1}) \simeq 2^{j_1(\alpha-F(2))} , \end{aligned}$$

which goes to 0 provided we choose $1 > \alpha > F(2)$. Thus $\bar{S}dM(j_1, 0)$ converges to $\tilde{K}K$ which proves (40).

Appendix E: Scaling properties of 1st and 2nd order scattering moments of MRW processes

The following theorem gives the MRW version of the Theorem 4.2 for MRM.

THEOREM E.1. *Let $X(t)$ be a Multifractal Random Walk as defined in (41) with integral scale 2^L and scaling exponents $\zeta(q)$. Then*

$$(100) \quad \forall j < L, \quad \tilde{S}X(j) = 2^{j \frac{3-\zeta(2)}{2}} ,$$

and if $\zeta(2) > 1$ then as long as $j_1, j_2 < L$, $\tilde{S}X(j_1, j_2)$ depends only on $j_1 - j_2$, and for each $j_2 < L$:

$$(101) \quad \lim_{j_1 \rightarrow -\infty} \tilde{S}X(j_1, j_2) = \tilde{K}$$

where the constant \tilde{K} is the constant of theorem 4.2 for the Multifractal Random Measure associated with $e^{\omega_t^L}$ in (41).

PROOF. The proof is very similar to the proof of Theorem 4.2 for MRM, so we only provide the main steps without entering into details.

First let us remark that if $\bar{\psi}(t) = \int_{-\infty}^t \psi(u)du$, then a simple integration by parts allows one to show that:

$$(102) \quad |X_l \star \psi_j| = 2^j |dX_l \star \bar{\psi}_j| ,$$

where $X_l(t)$ is defined in (41) and $dX_l(t) = l^{\frac{2-\zeta(2)}{2}} e^{\omega_l^{2L}(t)} dB(t)$. Then, in order to study the behavior of first and second order scattering moments of $X_l(t)$, one can adapt the proofs of the MRM case to the MRW case by replacing $e^{\omega_l(u)} du$ by $l^{\frac{2-\zeta(2)}{2}} e^{\omega_l^{2L}(u)} dB(u)$.

For the first order moment, the Wiener noise scaling $dB(su) \stackrel{law}{=} s^{-1/2} dB(u)$ and (38), leads to $dX_{sl}(su) \stackrel{law}{=} e^{\Omega_s} s^{1/2-\zeta(2)/2}$. Thanks to (102), one gets (100).

As far as the second order scattering moment is concerned, a simple adaptation of Lemma C.2 allows one to follow the same steps as in Appendix D. One is lead to the same decomposition as in (95):

$$(103) \quad \lim_{l \rightarrow 0} \psi \star |\psi_{j_1} \star X_l|(0) \stackrel{law}{=} e^{\Omega_{2^{-L}}} (I + II + III) ,$$

where

$$(104) \quad I = \tilde{K}' 2^{j_1 \frac{3-\zeta(2)}{2}} \int \psi(-u) e^{\omega_{2^{j_1} \alpha}(u)} du ,$$

$$(105) \quad II = 2^{j_1} \int \psi(-u) e^{\omega_{2^{j_1} \alpha}(u)} \bar{\epsilon}_{2^{j_1}(\alpha-1)}(2^{-j_1} u) du ,$$

$$(106) \quad III = 2^{j_1} \int \psi(-u) \bar{\eta}'_{j_1}(u) du ,$$

where $\bar{\eta}'_j$ is the noise term corresponding to η_j in Lemma C.2 and

$$\tilde{K}' = \mathbf{E} \left(\left| \lim_{l \rightarrow 0} \int \bar{\psi}(u) l^{\frac{2-\zeta(2)}{2}} e^{\omega_l^1(u)} dB(u) \right| \right) .$$

Since from (93),

$$\mathbf{E} \left(\left| \lim_{j_1 \rightarrow -\infty} \int \psi(-u) e^{\omega_{2^{j_1} \alpha}(u)} du \right| \right) = \tilde{K} ,$$

the term $\mathbf{E}(|I|)$ behaves, when $j_1 \rightarrow -\infty$ as $\tilde{K}' \tilde{K} 2^{\frac{3j_1-\zeta(2)}{2}}$. The contribution of the terms II and III can be shown to be negligible following the same arguments as in Appendix D. Since the first order scattering moment behaves like $\tilde{K}' 2^{j_1 \frac{3-\zeta(2)}{2}}$ we obtain (101) with the same constant as in Theorem 4.2. \square

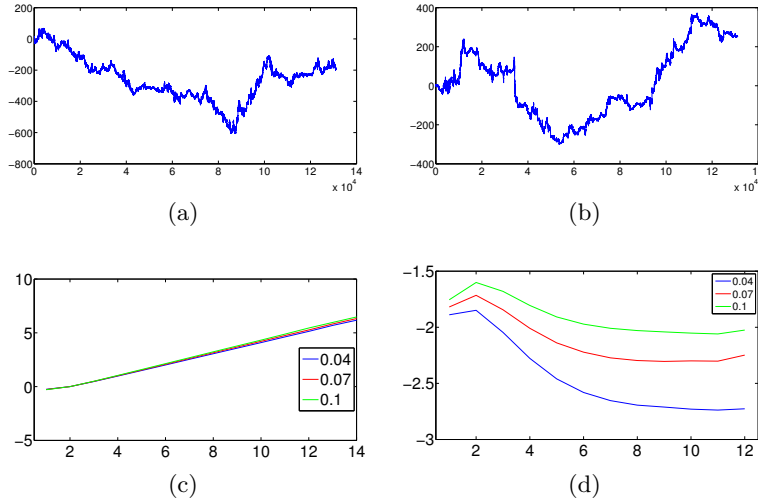


FIG 10. (a,b) Realizations $X(t)$ of log-normal Multifractal Random Walks with $\lambda^2 = 0.04$ and $\lambda^2 = 0.1$. (c) $\log_2 \tilde{S}X(j_1)$ with $\lambda^2 = 0.04$, $\lambda^2 = 0.07$ and $\lambda^2 = 0.1$. (d) $\log_2 \tilde{S}X(j_1, j_1 + l)$, for $\lambda^2 = 0.04$, $\lambda^2 = 0.07$ and $\lambda^2 = 0.1$, as a function of l , for $j_1 + l < L$ where $2^L = 2^{13}$ is the integral scale.

Figure 10 shows the scattering moments of multifractal random walks $X(t) = B(dM(t))$ for a log-normal random measure dM , with $\lambda^2 = 0.04$, $\lambda^2 = 0.07$ and $\lambda^2 = 0.1$. In the log-normal case, it results from (43) that

$$(107) \quad \zeta(q) = (1 + 2\lambda^2) \frac{q}{2} - \frac{\lambda^2}{2} q^2 ,$$

Thereby $\zeta(2) = 1$. As expected from (100), Figure 10(c) shows that $\log_2 \tilde{S}X(j_1) = j_1(\frac{3-\zeta(2)}{2})$. As expected from (101), Figure 10(d), compared to Figure 6(d), shows that second order scattering moments satisfy $\tilde{S}X(j_1, j_2) \approx \tilde{S}dM(j_1, j_2)$, for the three values of λ^2 . If one uses the same wavelet ψ , we check that they converge to the same constant \tilde{K} as in the MRM case which is proportional to the intermittency parameter λ : $\tilde{K} \approx 0.82 \lambda$ in the displayed examples.

Appendix F: Proof of Theorem 5.1

The Fourier transform $\Psi(\omega)$ of ψ satisfies the Littlewood-Paley condition (3)

$$\sum_{j=-\infty}^{\infty} \left(|\Psi(2^j \omega)|^2 + |\Psi(-2^j \omega)|^2 \right) = 2 .$$

It results that

$$(108) \quad |\Phi(2^M\omega)|^2 + \frac{1}{2} \sum_{j=-\infty}^M \left(|\Psi(2^j\omega)|^2 + |\Psi(-2^j\omega)|^2 \right) \leq 1 .$$

Let Y be a stationary process with $E(|Y(t)|^2) < \infty$, and $P_Y(\omega)$ be its power spectrum. Multiplying (108) by $P_Y(\omega)$ and integrating in ω gives

$$(109) \quad \mathbf{E}(|Y \star \phi_M|^2) + \sum_{j=-\infty}^M \mathbf{E}(|Y \star \psi_j|^2) \leq \mathbf{E}(|Y|^2) .$$

Let us prove by induction that for any $q \geq 2$

$$(110) \quad \mathbf{E}(|\widehat{S}X(j_1)|^2) + \sum_{m=2}^{q-1} \sum_{-\infty < j_2, \dots, j_m \leq M} \mathbf{E}(|\widehat{S}X(j_1, \dots, j_m)|^2) + \sum_{-\infty < j_2, \dots, j_q \leq M} \mathbf{E}(|X \star \psi_{j_1} \star \dots \star \psi_{j_q}|^2) \leq \mathbf{E}(|X \star \psi_{j_1}|^2) .$$

Applying (109) to $Y = |X \star \psi_{j_1}|$ proves that (110) for $q = 2$. If (110) is valid for q we prove it for $q+1$ by applying (109) to each $Y = |X \star \psi_{j_1} \star \dots \star \psi_{j_q}|$. Taking the limit of (109) as q goes to ∞ proves (??).

If ψ has a compact support then one can verify that there exists ϕ having the same support as ψ , whose Fourier transform satisfies (45), with an equality on the Fourier transform modulus. Since $\mathbf{E}(\widehat{S}X(j_1, \dots, j_m)) = \overline{S}X(j_1, \dots, j_m)$, the mean-square estimation error at the scale 2^{j_1} satisfies

$$\epsilon(j_1) \leq \sigma^2(|X \star \psi_{j_1}|) - \sum_{m=2}^{\infty} \sum_{-\infty < j_2, \dots, j_m \leq M} |\overline{S}X(j_1, \dots, j_m)|^2 ,$$

which proves (46) \square .

References

- [1] P. Abry, P. Flandrin, M. Taqqu, and D. Veitch. Wavelets for the Analysis, estimation and synthesis of scaling data. *K. Park and W. Willinger eds*, 2000.
- [2] J. Anden and S. Mallat. Deep scattering spectrum. *Submitted to IEEE transactions of Signal Processing*, 2013.
- [3] A. Arneodo and S. Jaffard. L'Analyse Multi-fractale des Signaux. *Journal du CNRS*, 2004.
- [4] E. Bacry, A. Kozhemyak, and J. F. Muzy. Continuous cascade models for asset returns. *Journal of Economic Dynamics and Control*, 32:156–199, 2008.
- [5] E. Bacry, A. Kozhemyak, and J. F. Muzy. Log-normal continuous cascades: aggregation properties and estimation. application to financial time series. *Quantitative Finance*, 13:795–818, 2013.

- [6] E. Bacry and J.F. Muzy. Log-infinitely divisible multifractal process. *Comm. in Math. Phys.*, 236:449–475, 2003.
- [7] J. Bruna and S. Mallat. Invariant scattering convolution networks. *IEEE transactions of PAMI*, 2012.
- [8] B. Castaing. Lagrangian and eulerian velocity intermittency. *Eur. Phys. J. B*, 29:357–358, 2002.
- [9] O. Chanal, B. Chabaud, B. Castaing, and B. Hebral. *Eur. Phys. J. B*, 17:309–317, 2000.
- [10] V. Chudacek, J. Anden, S. Mallat, P. Abry, and M. Doret. Scattering transform for intrapartum fetal heart rate variability fractal analysis: a case-control study. *IEEE Trans. on Biomedical Engineering*, to appear, 2013.
- [11] A. DasGupta. *Asymptotic Theory of Statistics and Probability*. Springer, 2008.
- [12] J. Delour, J. F. Muzy, and A. Arneodo. Intermittency of 1d velocity spatial profiles in turbulence : a magnitude cumulant analysis. *Eur. Phys. J. B*, 23:243, 2001.
- [13] U. Frisch. *Turbulence*. Cambridge University Press, 1995.
- [14] L. P. Hansen. Large sample properties of generalized method of moments estimators. *Econometrica*, 50:1029–1054, 1982.
- [15] S. Jaffard. Multifractal Formalism for functions, parts i and ii. *SIAM J. Math Anal.*, 1997.
- [16] S. Jaffard. Wavelet Expansions, Function Spaces and Multifractal Analysis. 2000.
- [17] S. Jaffard and Y. Meyer. Wavelet Methods for Pointwise Regularity and Local Oscillations of Functions. *Memoirs of the AMS*, 1996.
- [18] J.P. Kahane and J. Peyriere. *Sur certaines martingales de B. Mandelbrot*. Departement de mathematique, 1975.
- [19] A.N. Kolmogorov. The local structure of turbulence in incompressible viscous fluid for very large reynolds numbers. *Dokl. Akad. Nauk. SSSR*, 30:301, 1941.
- [20] A. Kyprianou. *An Introduction to the Theory of Lévy Processes*. 2007.
- [21] Y. LeCun, K. Kavukcuoglu, and C. Farabet. Convolutional networks and applications in vision. *Proc. IEEE Int. Symposium Circuits and Systems*, 2010.
- [22] S. Mallat. Group Invariant Scattering. *Communications in Pure and Applied Mathematics*, 2012.
- [23] B.B. Mandelbrot. On Intermittent Free Turbulence. *Turbulence of Fluids and Plasmas*, 1969.
- [24] B.B. Mandelbrot. Intermittent Turbulence in self-similar Cascades: divergence of high moments and dimension of the carrier. *Journal of Fluid Mechanics*, 1974.
- [25] B.B. Mandelbrot. *Fractals and scaling in finance. Discontinuity, concentration, risk*. Springer, 1997.
- [26] D. McFadden. A method of simulated moments for estimation of discrete response models without numerical integration. *Econometrica*, 57:995–1026, 1989.
- [27] C. Meneveau and K.R. Sreenivasan. The Multifractal nature of Turbulent energy dissipation. *J. Fluid Mechanichs*, 224:429–484, 1991.
- [28] J-F. Muzy, E. Bacry, and A. Arneodo. Multifractal Formalism for fractal signals: The structure-function approach versus the wavelet-transform modulus-maxima method. *Phys. Rev E*, 47:875, 1993.
- [29] J-F. Muzy, E. Bacry, and A. Arneodo. Singularity Spectrum of Fractal signals from wavelet analysis: exact results. *J. Stat. Phys*, 70:635, 1993.
- [30] J. F. Muzy, J. Delour, and E. Bacry. *Eur. J. Phys. B*, 17:537–548, 2000.
- [31] J.F. Muzy and E. Bacry. Multifractal stationary random measures and multifractal random walks using log-infinitely divisible laws. *Phys. Rev. E*, 66, 2002.
- [32] G. Oppenheim P.Doukhan and M. Taqqu. *Theory and Applications of Long-Range*

- Dependence*. Birkhauser, Boston, 2002.
- [33] L.F. Richardson. *Weather Prediction bt Numerical Process*. Cambridge Universtity Press, 1922.
 - [34] C. Robert and M. Rosenbaum. A new approach for the dynamics of ultra high frequency data: the model with uncertainty zones. *Journal of Financial Econometrics*, 9:344–366, 2011.
 - [35] R. Robert and V. Vargas. Gaussian multiplicative chaos revisited. *Annals of Probability*, 38(2):605–631, 2010.
 - [36] G. Selesnick, I. Baraniuk and Kingsbury N. A dual tree complex wavelet transform. *IEEE Signal Processing Magazine*, 123, 2005.
 - [37] L. Sifre and S. Mallat. Combined Scattering for Rotation Invariant Texture Analysis. *ESANN*, 2012.
 - [38] R. Vershynin. How close is the sample covariance matrix to the actual covariance matrix ? *Journal of Theoretical Probability*, 25(3):655–686, 2012.
 - [39] H. Wendt, P. Abry, and S. Jaffard. Bootstrap for empirical multifractal analysis. *IEEE Signal Proc. Mag.*, 24(4):38–48, 2007.
 - [40] H. Wendt, S.G. Roux, P. Abry, and S. Jaffard. Wavelet leaders and bootstrap for multifractal analysis of images. *Signal Proces.*, 89:1100–1114, 2009.
 - [41] A.M. Yaglom. The influence of fluctuation in energy dissipation on the shape of turbulent characteristics in the inertial interval. *Soviet Physics Dockl.*, 1966.

COURANT INSTITUTE OF MATHEMATICAL SCIENCES
DEPARTMENT OF COMPUTER SCIENCE
715 BROADWAY
NEW YORK, NY, 10012 E-MAIL: bruna@cims.nyu.edu

DEPARTEMENT D'INFORMATIQUE,
ÉCOLE NORMALE SUPÉRIEURE
45 RUE D'ULM
PARIS 75005 FRANCE E-MAIL: mallat@cmap.polytechnique.fr

CENTRE DES MATHÉMATIQUES APPLIQUÉES ,
ÉCOLE POLYTECHNIQUE
ROUTE DE SACLAY
PALAISEAU, FRANCE E-MAIL: bacry@cmap.polytechnique.fr E-MAIL: muzy@univ-corse.fr